

**Biological Comparison of DTPA and SCN-Benzyl-EDTA as Chelating Agents for Indium Labeling of Antibodies.**

Y. Arano, T. Mukai, T. Uezono, H. Motonari, K. Wakisaka, and A. Yokoyama. Faculty of Pharmaceutical Sciences, Kyoto University, Sakyo-ku, Kyoto 606, Japan.

Numerous bifunctional chelating agents (BCAs) have been developed to improve the radioactivity localization of Indium-111 (In) labeled antibodies in the liver when DTPA was used as a BCA. While these BCAs have provided lower hepatic radioactivity localization in animal studies (1, 2), high levels of radioactivity in the liver was still observed in clinical studies (3). These results suggest that factors other than *in vivo* instability of In chelate would also be responsible for the high radioactivity level in the liver. In this study, to compare the biological nature of radiolabeled metabolites derived from DTPA- and SCN-benzyl(Bz)-EDTA-In after lysosomal proteolysis in the liver, galactosyl-neoglycoalbumin (NGA) and mannosyl-neoglycoalbumin (NMA) were labeled with In using either BCA. NGA is known to be taken up by receptor-mediated endocytosis to the parenchymal cells of the liver, rapidly transported to lysosomal compartment, and then metabolized. Similar mechanism is also known between NMA and Kupffer cells of the liver (4, 5).

NGA and NMA were synthesized according to the procedure of Lee et al. (5) and labeled with In using DTPA anhydride or SCN-Bz-EDTA as the BCA (Fig. 1). Biodistribution of radioactivity after injection of In-labeled glycoalbumins in mice was examined. At 24 h post-injection, radioactivities in the liver, urine, and feces were analyzed by size-exclusion HPLC, reverse-phase HPLC, cellulose acetate electrophoresis and silica gel TLC.

In mice biodistribution studies, all the In-labeled neoglycoalbumins exhibited immediate and quantitative accumulation in the corresponding cells of liver. When NGA-DTPA-In was injected, more than 60 % of the injected radioactivity remained in the liver at 24 h post-injection with 18 % and 12 % of the radioactivities being excreted in the urine and feces, respectively. Also more than 60 % of the injected radioactivity was found in the liver over 24 h post-injection of NMA-DTPA-In with 15 % and 2 % of the radioactivities recovered in the urine and feces, respectively (Fig. 2). Analyses of the liver homogenate suggest that most of the radioactivity remained in both cells of the liver was identical and appeared to be lysine-DTPA-In. On the other hand, NGA-SCN-Bz-EDTA-In demonstrated rapid elimination of radioactivity from the liver with more than 80 % and 6 % of the radioactivities being excreted in the feces and urine, respectively at 24 h post-injection. However, 65 % of the radioactivity was retained in the liver at 24 h post-injection of NMA-SCN-Bz-EDTA-In with 29% and 8% of radioactivities excreted in the urine and feces, respectively (Fig. 3). Further analyses of the liver and feces ho-

mogenate and urine samples indicated that most of the radioactivity of each sample was found at the lysine-SCN-Bz-EDTA-In fraction.

The gathered results suggest that when DTPA or SCN-Bz-EDTA was used as a BCA for In radiolabeling, lysine-DTPA-In or lysine-SCN-Bz-EDTA-In appeared to be generated as the major metabolite after lysosomal proteolysis in both parenchymal and Kupffer cells of the liver, respectively. While the radiolabeled metabolite derived from DTPA-In displayed a very slow clearance from both cells of the liver, faster rate of radioactivity clearance from parenchymal cell was achieved with SCN-Bz-EDTA-In derived NGA. However, prolonged radioactivity localization was observed with this BCA from the Kupffer cells of liver. Thus, the present study indicates that biological characteristics of radiolabeled metabolite derived from each BCA are critical for the radioactivity clearance from both cells of the liver.

### References

- (1) Brechbiel MW, Gansow OA, Atcher RW, et al. *Inorg. Chem.* **25**, 2772-2781 (1986).
- (2) Deshpande SV, Subramanian R, McCall MJ, et al. *J. Nucl. Med.* **31**, 218-224 (1990).
- (3) Yokoyama K., Carrasquillo JA, Chang A, et al. *J. Nucl. Med.* **30**, 320-327 (1989).
- (4) Ashwell G and Haford J. *Ann. Rev. Biochem.* **51**, 531-554 (1982).
- (5) Lee YC, Stowell CP and Krantz MJ. *Biochemistry* **15**, 3956-3963 (1976).

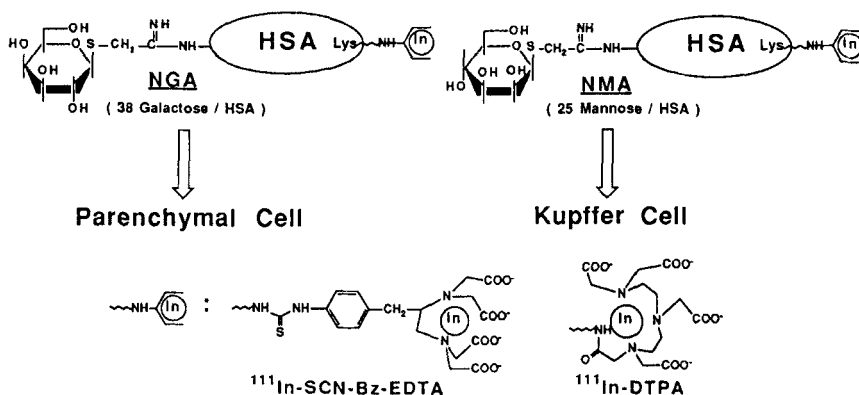


Fig. 1. Chemical structure of Indium-111 labeled galactosyl-neoglycoalbumin and mannosyl-neoglycoalbumin.

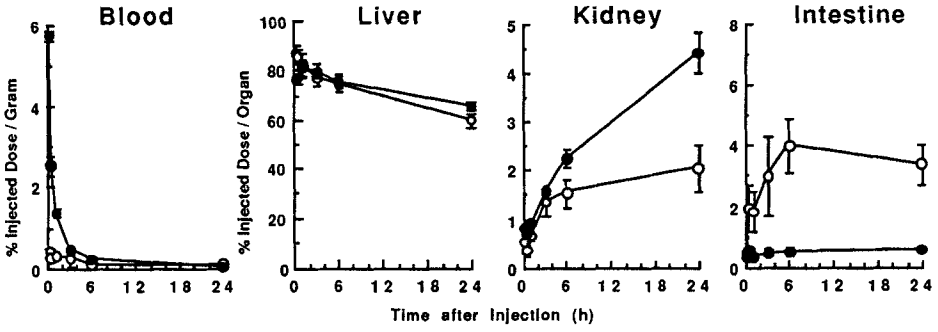


Fig. 2. Comparative radioactivity biodistributions after i.v. injections of NGA-DTPA-<sup>111</sup>In (O) and NMA-DTPA-<sup>111</sup>In (●) in normal mice.

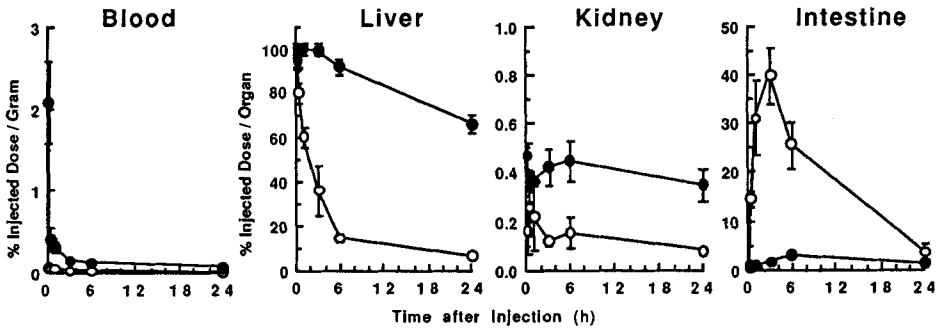


Fig. 3. Comparative radioactivity biodistributions after i.v. injections of NGA-SCN-Bz-EDTA-<sup>111</sup>In (O) and NMA-SCN-Bz-EDTA-<sup>111</sup>In (●) in normal mice.

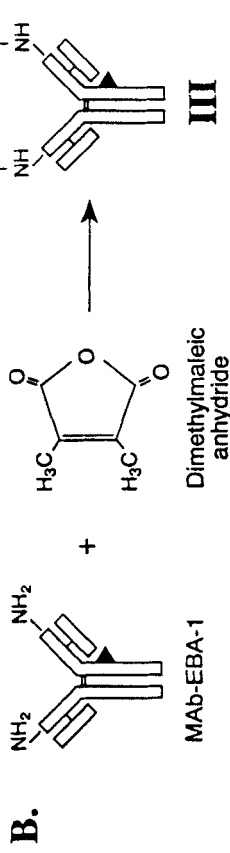
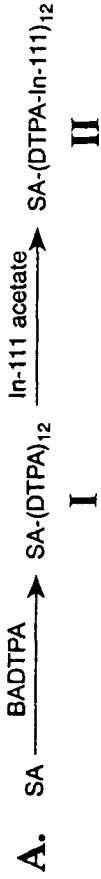
**A Novel Synthesis of MAb EBA-1-Oligosaccharide-BH-SA-DTPA-In-111 Using DMA as a Reversible Amino Group Protecting Agent.** Wang, TST; Yemul, S;

Fawwaz, RA; Van Heertum, RL; and Estabrook, A. College of Physicians and Surgeons, Columbia University, NY, NY

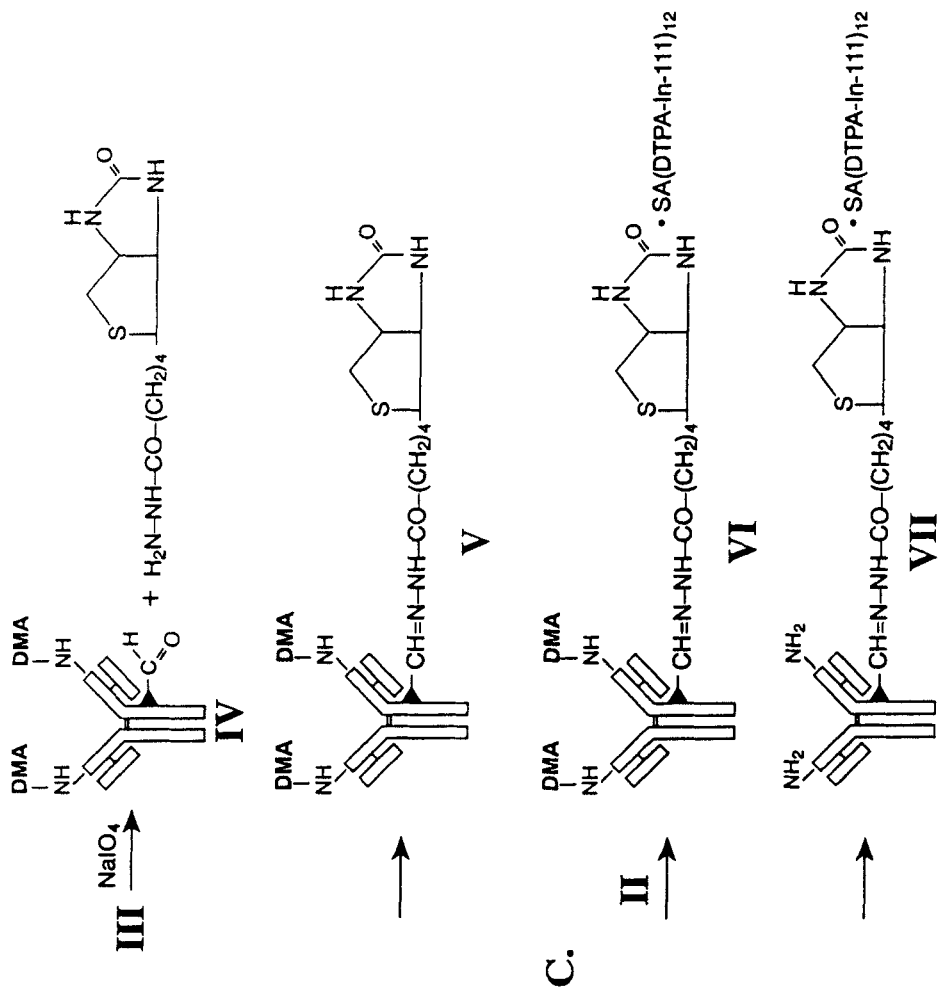
The aim of this study is to present a strategy to modify the oligosaccharide moieties of MAbs without sacrificing immunoreactivity. In this experiment, EBA-1, a MAb against human breast carcinoma associated antigen, was covalently conjugated to biotin hydrazide (BH)-Streptavidin (SA)-DTPA-In-111 (VI) using 2,3-dimethylmaleic anhydride (DMA) as a reversible amino group blocking agent. EBA-1 was reacted with DMA to form EBA-1-DMA (III), which was oxidized with NaIO<sub>4</sub> to yield the polyaldehyde-DMA-EBA-1.(IV). This was immediately reacted with BH to produce a stable biotin hydrazone (V). Separately, SA was treated with BADTPA to form SA-DTPAs, which was chelated with In-111 (II). (II) and (V) were combined to form (VI). Protecting groups were removed by dialysis in a pH 7.0 buffer solution yielding (VII). Compound (VIII) without DMA protecting groups was also prepared as a control. In direct cell binding experiment results, the immunoreactivity of VII was found to be about 20% higher than that of VIII, (69% vs. 58%).

Biodistribution in non-tumor rats showed the liver localization of VII to be about 50% lower than that of VIII at 24 and 48 hrs. post injection (1.34% vs. 3.83%, and 1.08% vs. 2.38%, respectively). The results demonstrate that 1) DMA can be used to protect NH<sub>2</sub> groups and prevent undesirable intra- or inter-molecular Schiff's Base formation during oxidation of the oligosaccharides of EBA-1; 2) the reaction product, a hydrazone, does not require stabilization with NaBH<sub>4</sub>, as do amino compounds; 3) the protecting groups can be easily removed in neutral buffer solution.

**Synthesis of MAb EBA-1-Biotin-Hydrazono-Streptavidin-DTPA-In-111 (VII)**



SA = Streptavidin	BADTPA = Bicyclic anhydride of DTPA
▶ = Oligosaccharide	DMA = $\text{H}_3\text{C} - \text{C} = \text{C} - \text{CH}_3$ $\quad \quad \quad  $ $\quad \quad \quad \text{CO} \quad \text{COOH}$



**A New Method of Labeling Monoclonal Antibodies with Indium-111 using DOTA-NHS as the Chelating Agent**

ZHOU, Y.G.; KHAZAELI, M.B.; and BUCHSBAUM, D.J.

Departments of Radiation Oncology and Medicine, University of Alabama at Birmingham, Birmingham, AL 35233.

Radiolabeled monoclonal antibodies (MoAbs) have been employed for radioimmunoimaging and radioimmunotherapy (1,2). For cancer imaging, indium-111 as a label has been investigated(3,4). Its advantages are that it has gamma energies of 173 keV and 247 keV to make it ideally suited for imaging, and it has a convenient half-life of 67.9 h. Labeling with indium-111 entails the attachment of a chelating agent to the antibody, and the conjugate is then able to bind indium-111. The use of the chelating agent 2-(p-nitrobenzyl)DOTA and its conjugation to the yttrium (III) complex has been reported by Moi et al.(5).

We explored the possibility of linking the bifunctional chelate DOTA-NHS with MoAb 17-1A and then labeling with indium-111. DOTA was reacted with N-hydroxysuccinimide (NHS) and N,N'-dicyclohexylcarbodiimide (DCC) in DMSO solvent at two different molar ratios: one was DOTA:NHS:DCC=1:1:1, and the other was DOTA:NHS:DCC=1:2:2. The DOTA-NHS/MoAb 17-1A molar ratio used was 50/1. DOTA-NHS was dissolved in DMSO at a concentration of 33.7  $\mu\text{g}/3.37 \mu\text{l}$ . The 17-1A MoAb concentration was 10 mg/1.5 ml, and 0.23 mg in a volume of 35  $\mu\text{l}$  was conjugated to DOTA-NHS. The conjugation buffer was 0.1 M  $\text{NaHCO}_3$  (pH 8.1). The 17-1A-DOTA-NHS conjugate was purified from free DOTA-NHS by passage through a column of Sephadex G-50.

The labeling reaction buffer was 0.5 M ammonium acetate (pH 6.0). The volume used was 40  $\mu\text{l}$ . One-hundred  $\mu\text{Ci}$   $\text{InCl}_3$  in 0.5 M ammonium acetate was added to 17-1A-DOTA in buffer solution. The labeling incubation time was 3-6 h at room temperature with slow stirring. The  $^{111}\text{In}$ -labeled 17-1A-DOTA was identified and separated by HPLC with a TSK-3000 gel filtration column. The radioactivity of the effluent was continuously determined by a flow-through radioisotope detector. The average labeling efficiency was 30% when the DOTA:NHS:DCC molar ratio was 1:1:1, and it was 40% when the DOTA:NHS:DCC molar ratio was 1:2:2.

In summary, a new bifunctional chelating agent (DOTA-NHS) has been synthesized and used successfully for the labeling of MoAb 17-1A with indium-111. In the future, we will study the immunoreactivity of such conjugates and their biodistribution in animal tumor xenograft models.

References:

1. Gansow, O.A. Nucl. Med. Biol. 18, 369-381 (1991)
2. Parker, D. Chem. Soc. Rev. 19, 271-291 (1990)
3. Ruser, G.; Ritter, W. and Maecke, H.R. Bioconjugate chem. 1, 345-349 (1990)
4. Wu, C.; Virzi, F. and Hnatowich, D.J. Nucl. Med. Biol. 19, 239-244 (1992)
5. Moi, M.K.; Meares, C.F. and DeNardo, S.J. J. Am. Chem. Soc. 110, 6266-67 (1982)



**Production and Use of Cobalt-55 as an Antibody Label for PET Imaging**

SRIVASTAVA, S.C.; MAUSNER, L.F.; KOLSKY, K.L.; MEASE, R.C.; JOSHI, V; MEINKEN, G.E.; PYATT, B; WOLF<sup>1</sup>, A.P.; SCHLYER<sup>1</sup>, D.J.; LEVY<sup>1</sup>, A.V.; and FOWLER<sup>1</sup>, J.S. Medical and <sup>1</sup>Chemistry Department, Brookhaven National Laboratory, Upton, NY 11973

PET imaging can enhance the diagnostic and therapeutic usefulness of radiolabeled monoclonal antibodies (MAB) by providing more quantitative information on biodistribution and pharmacokinetics, and dosimetry. This study was undertaken to develop Co-55 [ $t_{1/2}$  17.5h;  $\beta^+$  max 1500 keV, 77%;  $\gamma$  511 keV (152%), 477 keV (16%), 931 keV (73%)] as a positron emitter label for MABs (1). The production of very pure no-carrier-added (NCA) Co-55 has been achieved using the Fe-56 (p,2n) reaction. Targets consisted of high-purity natural iron foils (25mm x 25mm, 0.33mm thickness) and were irradiated both at the Brookhaven National Laboratory (BNL) cyclotron, with 28 MeV protons, and at the Brookhaven Linac Isotope Producer (BLIP) with 40 MeV protons. At end-of-bombardment (EOB), Co-55 thick-target yields (TTY) at 28 MeV were 919  $\mu\text{Ci}/\mu\text{Ah}$ . At 40 MeV, Co-55 TTY at EOB were 335  $\mu\text{Ci}/\mu\text{Ah}$ . These results are consistent with published excitation functions. Typical four-hour irradiations at 28 MeV produced 10.2 mCi Co-55/g Fe with 64  $\mu\text{Ci}$  Co-56 in the cyclotron vs. 9.1 mCi Co-55/g Fe with 123  $\mu\text{Ci}$  Co-56 at BLIP (40 MeV). A radiochemical separation based on solvent extraction with methyl-isobutyl ketone (MIBK) was developed to purify the NCA Co-55 from the iron target. MIBK was superior in terms of the Fe/Co separation factor achievable and separation time, compared to the more commonly used solvent, isopropyl ether. Gradient elution with HCl on an anion exchange column (Dowex 1-X8, 100-200 mesh, 15 mL column volume) was used to further purify the product from both trace stable iron and Mn-52,54 and Cr-51 radioisotopes co-produced in the irradiations. Cobalt recovery was 90% in approximately 5 h. Less than 2 ppm Fe or Co were detected in the final product from spectrophotometric analysis.

To determine if the 477 and 931 keV emissions would interfere with PET imaging, images of a modified Jaszczak phantom, filled with an aqueous solution of Co-55-EDTA, were obtained using the CTI 931 whole body PET scanner at BNL. The image resolution was found to be quite satisfactory (Figure 1). Evaluation of previously developed bifunctional chelating agents (BCA) (2) showed that two semi-rigid polyaminocarboxylate ligands, cyclohexyl EDTA monoanhydride (CDTA-MA), and 4-isothiocyanato-trans-1,2,-diaminocyclohexane N,N',N'-tetraacetic acid (4-ICE) produced stable cobalt immunoconjugates (Co-57,  $t_{1/2}$  270d, used for convenience). 4-ICE was selected for further study with Co-55. The commonly used BCA, DTPA-dianhydride (DTPA-DA), was used as a control ligand. Labeling was typically accomplished by adding  $\sim 10\mu\text{l}$  Co-55  $\text{Cl}_2$  (0.5-5mCi) in 0.1M HCl to  $\sim 500\mu\text{g}$  of the conjugate (1.5-3.0 BCA/MAB), 0.1M acetate buffer, pH 5.5, and incubating for 2-4h at 25°C. The mixture, following EDTA challenge, was purified by size exclusion HPLC to give the labeled monomeric conjugate. Labeling yields were  $90 \pm 5\%$ , the in-vitro serum stability at 4d ranged between 90 and 100%, and the retention of immunoreactivity was  $80 \pm 10\%$ . In nude mice xenografted with LS-174T human tumor cells, tumor (T) uptake (% injected dose per g) of Co-55 conjugates at 24 and 48h respectively, was as follows: 4-ICE, 25.2 and 17.7; DTPA-DA, 9.0 and 4.9 (Table 1). The tumor to blood (B), liver (L), and kidney (K) ratios, at 24 and 48h, respectively, were: 4-ICE, T/B 4.4 and 9.3, T/L 4.3 and 5.1, T/K 3.6 and 4.5; DTPA-DA, T/B 3.2 and 5.4, T/L 1.3 and 1.1, T/K 2.1 and 1.6 (Table 2). Our results

demonstrate that high-purity NCA Co-55 can be produced in good quantity and that it is suitable for PET imaging. Using 4-ICE for conjugation, Co-55 should be potentially useful as a positron emitter label for monoclonal antibodies.

1. Srivastava, S.C.; Mease, R.C.; Meinken, G.E.; et al., *J. Nucl. Med.* 30:923 (1989) (Abst.)
2. Mease, R.C.; Meinken, G.E.; Chinol, M.; et al., *J. Nucl. Med.* 33:985 (1992) (Abst.)

This work was supported by the U.S. Department of Energy under Contract No. DE-AC02-76CH00016. Thanks are due to J. C. Saccavini, Compagnie ORIS Industrie, Gif Sur Yvette, France, for providing the anti-CEA antibody used in these studies.

**Table 1. Biodistribution (% Dose/g) of  $^{55}\text{Co}$  Labeled Anti-CEA  $\text{F}(\text{ab}')_2$  Immunoconjugates in Nude Tumor Mice\***

Ligand	Time (Hr)	Tumor	Blood	Liver	Kidney	Whole Body (% Dose)
DTPA-DA	24	9.02 ± 1.55	2.84 ± 0.25	7.00 ± 0.82	4.41 ± 0.19	39 ± 3
		---	(3.2)	(1.3)	(2.1)	
	48	4.87 ± 0.42	0.91 ± 0.08	4.49 ± 0.40	3.04 ± 0.13	23 ± 0.6
		---	(5.4)	(1.1)	(1.6)	
4-ICE	24	25.19 ± 2.56	5.71 ± 0.95	5.86 ± 0.28	7.07 ± 0.41	59 ± 1.5
		---	(4.4)	(4.3)	(3.6)	
	48	17.72 ± 2.84	1.90 ± 0.46	3.50 ± 0.53	3.92 ± 0.39	37 ± 3
		---	(9.3)	(5.1)	(4.5)	

\*LS-174T tumor xenografts; n = 5. Tumor to organ ratios in parentheses

**Table 2. Improvement in Tumor/Organ Ratios of  $^{55}\text{Co}$  anti-CEA  $\text{F}(\text{ab}')_2$  Immunoconjugates\***

Ratio, Tumor To:	DTPA-DA		4-ICE		Improvement Factor 4-ICE/DTPA-DA	
	24 h	48 h	24 h	48 h	24 h	48 h
Blood	3.2	5.4	4.4	9.3	1.4	1.7
Liver	1.3	1.1	4.3	5.1	3.3	4.6
Kidney	2.1	1.6	3.6	4.5	1.7	2.8
% dose per g in tumor	9.0	4.9	25.2	17.7	2.8	3.6

\* LS-174T tumor xenografts in nude mice

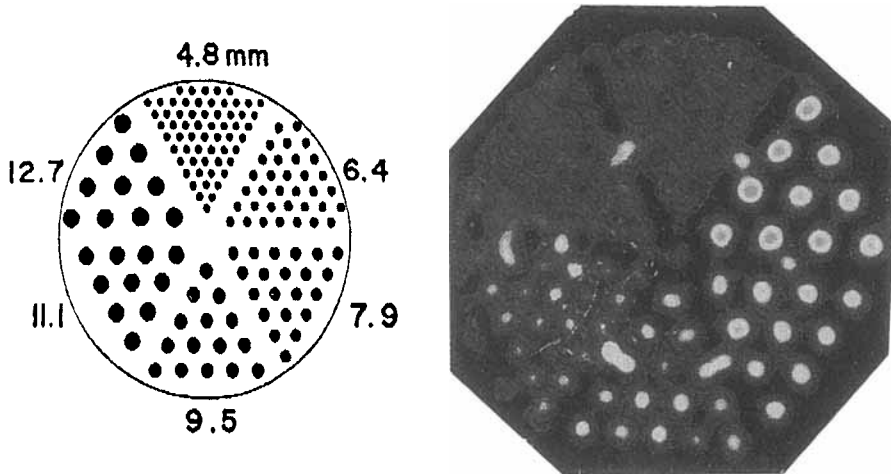


Figure 1. A typical image (mirror image, right) of a modified Jaszczak phantom (shown schematically, left) filled with an aqueous solution of  $^{55}\text{Co}$ -EDTA. The phantom consists of 6 sets of hollow channels (diam: 4.8, 6.4, 7.9, 9.5, 11.1, 12.7 mm) with center to center spacings of channels of 2 times the diameter. Images were made using the CTI 931 whole body PET scanner at BNL.

**A New Three-Step Strategy Using the Avidin-Biotin System for Radioimaging Tumours.**

SMITH S.V.\*; VAN DEN ABEELE, A.D.#; BARANOWSKA-KORTYLEWICZ, J.#; JONES, P.L.#; LAMBRECHT, R.M.\*; ADELSTEIN, S.J.#; and KASSIS, A.I.#. Harvard Medical School#, Boston, MA 02115, USA and Biomedicine and Health Program\*, ANSTO, Lucas Heights 2234, Sydney, Australia.

Radiolabelled monoclonal antibodies (MAb) for the detection of cancer have been extensively studied. However, the delivery of the radiolabel to the target site and the target to nontarget ratios are still far from optimal. More recently, attention has been focused on the use of the high affinity avidin-biotin system in two- and three-step procedures for radioimmunodiagnosis and radioimmunotherapy of cancers.<sup>1-4</sup> Such procedures hold promise for amplification at the target site, faster clearance of the radiolabel, and reduced exposure of nontarget organs.

A new three-step procedure for the radioimaging of the tumours is described in which a biotinylated derivative of B72.3 monoclonal antibody was injected intravenously into nude mice bearing LS174T colon carcinoma, followed by consecutive administration of avidin and biotinylated, radioiodinated human serum albumin (HSA) at 48-hour intervals.

As it was important to maintain the immunoreactivity of the antibody, the protein was biotinylated at low protein:biotin ratios using biotinyl-N-hydroxysuccinimide ester (BNHS) in carbonate buffer (0.1 M bicarbonate, 0.2 M NaCl, pH 8.5) (see Scheme 1). The number of biotin groups per protein molecule was determined using <sup>3</sup>H-BNHS. The immunoreactivity of each species was assessed by an indirect radioimmunoassay and found to be comparable to that of the unreacted antibody. A Scatchard plot demonstrated that the interaction between the biotin molecules on the antibody and streptavidin was cooperative.

**Biotinylation of Antibody**

MAb	+	nBNHS	=	MAb-B <sub>m</sub>
		n		m
		3		0.8
		8		2.0
		18		4.0

**Scheme 1**

The preparation of the radiolabelled, biotinylated HSA involved iodination of HSA in the presence of Iodogen followed by purification of the protein on a Sephadex-G25 column. The isolated, radiolabelled protein was then reacted with BNHS in carbonated buffer (0.05 M, pH 8.5) for 30 minutes. Unreacted BNHS was removed by a size exclusion cartridge and the protein resuspended in phosphate buffered saline.

Two animal biodistribution studies were conducted. Study A involved the injection of the MAb -B<sub>4</sub> (55 µg) followed by intraperitoneal injection of avidin (100 µg) on day 3. On day 5 the radiolabelled, biotinylated HSA (I-HSA-B<sub>9</sub>) was injected and 22 hours later the animals were killed, dissected, and the organs were counted in a gamma counter. In Study B the animals were injected with MAb-B<sub>1</sub> (25 µg) followed by avidin and radiolabelled biotinylated HSA (I<sub>10</sub>-HSA-B<sub>9</sub>) at consecutive 48-hour intervals. Control animals received the radioiodinated HSA only.

The data are shown in Figure 1. Tumour uptake after 22 hours was  $0.97 \pm 0.48$  %ID/g and  $1.09 \pm 0.25$  %ID/g for Study A and Study B, respectively. Liver uptake in Study B ( $1.35 \pm 0.35$  %ID/g) was much higher than that in Study A ( $0.41 \pm 0.35$  ID/g) was much higher than that in Study A ( $0.41 \pm 0.1$  %ID/g), while tumour uptake for each set of controls was comparable (0.52-0.59).

The results indicated that the three-step approach described may be useful in increasing target/nontarget ratios and reducing total dose to nontarget tissues.

1. Goodwin, D.A. - *J.Nucl.Med.* 33: 1816 (1992)
2. Paganelli, G., Malcoati, M., and Fazio, F. - *Nucl.Med.Comm.* 12: 211 (1991).
3. Paganelli, G., Magnani, P., Zito, F. et al. - *Cancer Res.* 51: 5960 (1991).
4. Hnatowich, D.J., Virzi, F., and Rusckowski, M. - *J.Nucl.Med.* 28: 1294 (1987).

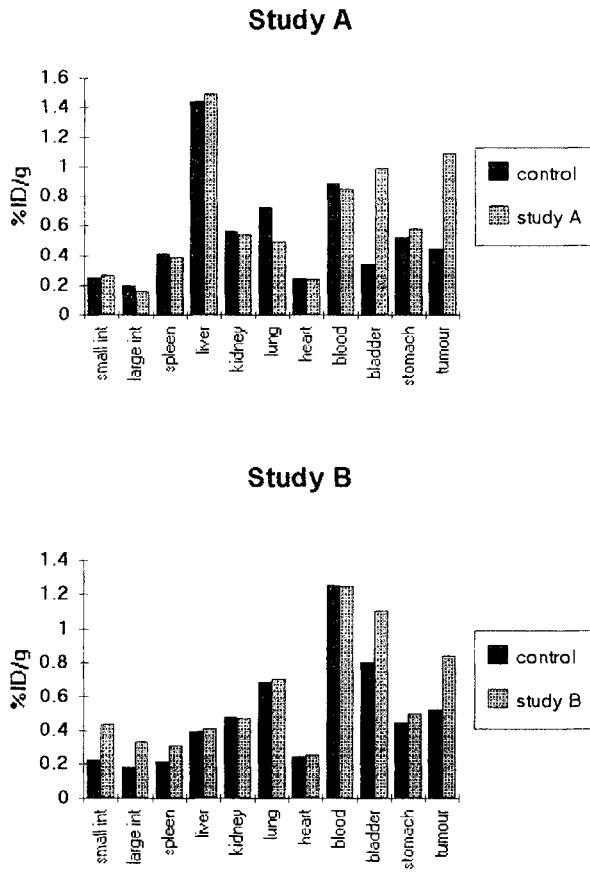


Figure 1. Biodistribution Data



### Complexation

6. Add 0.5  $\mu\text{l}$  of 5 mM Sn(II)-tartrate and 1 GBq [ $^{99\text{m}}\text{Tc}$ ]pertechnetate, leave for 5 minutes and determine free pertechnetate by ITLC (10 min).
7. Ultracentrifuge, if necessary, and filter sterile (20 min.).

The time necessary for the single steps is indicated in parentheses. Therefore, a technician needs less than two hours for the conjugation and an additional time period of 30 minutes for complexation including a purification step, if necessary. For routine applications step 1 can be performed in advance reducing the total preparation time to about one hour.

The ultracentrifugation technique used here for purifying  $^{99\text{m}}\text{Tc}$  labeled BAT-antibodies from side reacted NHS-BAT ester<sup>3</sup> and from unreacted [ $^{99\text{m}}\text{Tc}$ ]pertechnetate are the key steps for an easy to perform conjugation/labeling procedure of proteins. Using the indicated ultracentrifugation tubes with each step the volume is reduced from 2.5 to 0.25 ml within 15 minutes thus decreasing contaminants to 10% of their initial concentration. Even in case the complexation yield deviates from normally achieved >90%, the purification by step 7 provides a  $^{99\text{m}}\text{Tc}$  labeled antibody with 1/10 of the original impurity like [ $^{99\text{m}}\text{Tc}$ ]pertechnetate. Thus purification and complexation yield determination is furnished by the final step (7).

After conjugation the BAT-antibody can either be used for immediate complexation or stored for future application. Since the mercaptogroups of the BAT ligand tend to close slowly to disulfides by intramolecular oxidation the conjugate must be stored in a freezer or lyophilized and kept under inert atmosphere. After complexation the label is stable for more than 24 hours. The amount of [ $^{99\text{m}}\text{Tc}$ ]pertechnetate liberated depends on the number of conjugated BAT ligands. The amount of free [ $^{99\text{m}}\text{Tc}$ ]pertechnetate was < 5% after 24 hours after binding 4 BAT-ligands/IgG.

The immunoreactivity of the anti CEA antibody (BW 431/26) which was used in these experiments did not suffer from any of the indicated conjugation steps. Additionally, as demonstrated in the figure below, a BAT-ligand load of up to 9.6 BAT ligands bound per IgG molecule did not reduce the antigen binding significantly at high cell concentrations. With increasing dilution, however, the binding decreased with increasing BAT load reflecting some reduction of affinity. In respect to the immunoreactivity and the  $^{99\text{m}}\text{Tc}$  labeling yield the optimal BAT ligand number bound per antibody is therefore considered to be around 4 BAT ligands/IgG. Positive radioimmunoscintigraphy of patients with recurrent colorectal carcinoma using  $^{99\text{m}}\text{Tc}$  labeled BAT-BW 431/26 proved the clinical value of the introduced conjugation method.

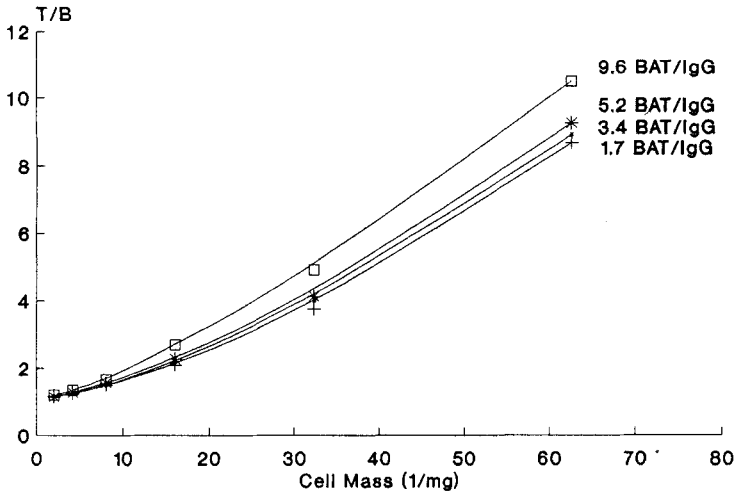
### References

1. Kasina S., Rao T.N., Srinivasan A. et al. - J.Nucl.Med. 32: 1445 (1991)
2. Eisenhut M., Mißfeldt M., Lehmann W.D. et al. - J.Labelled Comp. Radiopharm. 29: 1283 (1991)
3. Eisenhut M., Lehmann W.D. - J.Labelled Comp. Radiopharm. 32: in press (1993)

Financial support from the Deutsche Forschungsgemeinschaft is gratefully acknowledged.



Antigen Binding of Tc-99m-BAT BW 431/26  
as a Function of BAT Load



USE OF FORMAMIDINE SULFINIC ACID FOR DIRECT Tc-99m LABELING OF IgG ANTIBODY.

X.B.WANG.; A.A.NOIJAIM.\*; and T.R.SYKES.\* Department of Chemistry, Beijing Normal Univ. Beijing, China. \*Faculty of Pharmacy, Univ. of Alberta. Edmonton Canada T6G 2N8

Formamidine sulfinic acid (1) is known as a useful reducing agent for both inorganic and organic compounds. A study of the redox potential of formamidine sulfinic acid as a function of concentration and pH gave a value of  $-1.5$  volts for the pH range 4–8 at concentration levels of  $4 \times 10^{-4}$ – $1 \times 10^{-2}$ M. One major advantage of formamidine sulfinic acid as a biochemical reducing agent is that both the reduced and oxidized (sulfonic acid) forms of the compound are water soluble and optically transparent above  $300\text{m}\mu$ . This reductant avoids some of the problems which may result from the tendency of stannous salts to hydrolysis and oxidation.

For Tc-99m labeling of IgG antibodies, two general approaches have been developed. One approach uses direct labeling (2) the other approach uses bifunction chelates (3.). Direct labeling is more economical. It is achieved when some of the disulfide bonds of the antibody are reduced to sulfhydryl groups. These sulfhydryl groups provide sites for the formation of very strong bonds between the reduced technetium and the antibody. In this paper, we used 6 mg or lower than that amount of FSA as a reducing agent for IgG antibody labeling with Tc-99m.

The antibody was first changed from buffer into saline and concentrated to about 10 mg/ml by ultra-filtration. The IgG antibody (2mg) in saline was pretreated by reaction with a appropriated buffer solution and FSA as a reducing agents at  $39\text{--}40^\circ\text{C}$  for 2 hr and then adding Tc-99m for labeling. (Table1. 2.)

Radiochemical purity and in vitro stability were measured by a combination of

ITLC. TCA and stable labeling methods. Two develop systems in acetone and in methanol: ammonia acetate (10% in water) = 1:1 (V/V) were used for the ITLC. For determination of Tc-99m IgG antibody levels, strips were air dried. After finishing the strip development, it was removed and cut into two parts, with each part of the strip dropped into separated test tubes. The relative counting rates of the two parts of the strip were measured in a gamma scintillation counter. The percent of IgG antibodies bound Tc-99m was calculated as the percent of the radioactivity on the bottom part of the strip.

Several challenge solutions were prepared for Transchelation Challenge Test (Fig.1). The challenge solutions were as follows: (1) 0.003M EDTA, (2) Phosphate buffered saline, (3) The fresh cysteine solution of a different concentration. At the end of labeling IgG, the Tc-99m IgG was separated from the reducing agents (FSA) by passage through a Sephadex G-50 column with collection of only that volume of solution which contained the protein.

Table 3 Show the results for The assay of immunoreactivity of the reduced and labeled antibody (Mab170).

We reported use of FSA for direct Tc-99m labeling of IgG antibody, results suggest that the method provides a direct and efficient means of labeling IgG antibody with Tc-99m and offers the possibility of performing labelling by a kit.

TABLE 1. LABELING YIELD OF Tc-99m IgG PREPARED WITH FSA METHOD

No.	Labeling	TLC-A % bound	TLC-M.N % bound	TCA % bound
1	Tc-99m	98.0	89.6	90.9
2	"	97.2	92.0	91.1

\*A=acetone M.N=methanol: ammonia acetate

TABLE 2. MAb170 LABELING WITH Tc-99m USING FSA METHOD

No.	Labeling	TLC-A % bound	TLC-M.N % bound	TCA % bound
1	Tc-99m	98.2	95.0	92.7
2	"	94.7	82.8	81.4

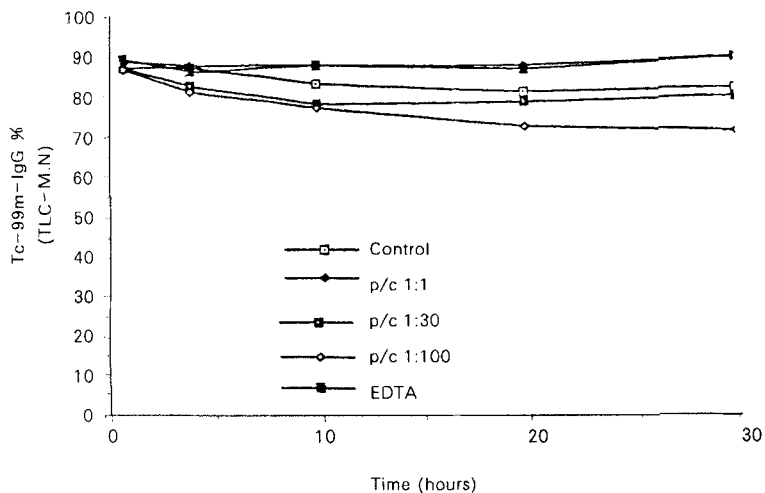


Fig.1. Transchelation challenge of purified Tc-99m IgG with cysteine and EDTA using FSA method

TABLE 3. THE ASSAY OF IMMUNOREACTIVITY OF THE REDUCED AND Tc-99m LABELED ANTIBODY (MAb170)

Sample Conc. ng	STD170 % INHIB	*1 % INHIB	*2 % INHIB
40	92.19	91.47	91.10
20	83.39	80.63	83.26
10	65.54	61.90	66.26
5	45.93	31.10	47.10
2.5	24.58	26.50	31.44

## REFERENCES

1. Shashoua VE.- *Biochem.*3: 1719. (1964)
2. Rhodes BA, et al.- *J. Nucl. Med.* 21:54 (1980)
3. Krejcarek GE and Tucker KL.- *Biochem. Biophys. Res. Commun.* 77: 581 (1977)

**Tc-99m Labeled Monoclonal Antibodies:**

**Structural variations by reduction mediated and BFCA Techniques**

John, E.<sup>1</sup>, Baum, R.<sup>2</sup>, Thakur, M.L.<sup>1</sup>

1. Thomas Jefferson University, Philadelphia, PA 19107.
2. Frankfurt University Germany.

A large array of monoclonal antibodies (MAbs) are labeled with Tc-99m by either the disulfide reduction or the bifunctional chelating agent (BFCA) technique. Three reducing agents, stannous chloride (SnCl<sub>2</sub>), 2-Mercapto ethanol (2-ME) and Ascorbic Acid (AA) have been commonly used (1-3). These do differ, however, in their reduction potentials, proportions to the MAbs, periods of incubation and chemical conditions used. Bifunctional chelating agents are also employed to label MAbs with Tc-99m at different conditions(4,5). All these procedures can result in structural perturbations, may alter in vivo distribution and may even affect the immunoreactivity of MAbs.

Hnatowich et al (6) and Fritzberg et al (7), for example, have performed a limited comparison between MAbs labeled with Tc-99m by the reduction mediated direct method and BFCA methods and reported some important differences in tissue distribution of the agents prepared by the two methods.

Human polyclonal immunoglobulin (HIgG Sandoz) was used as a model protein, and labeled with Tc-99m by the AA reduction technique (3) and also by the c-DTPA and N,N,N',N'-tetrakis (2-Mercapto ethyl) ethylene diamine(N<sub>2</sub>S<sub>4</sub>) BFCA methods (8,9). HIgG-SnCl<sub>2</sub> and BW 250/183-ME kits were gifts from RhoMed, Inc. and Dr.Baum, respectively, and labeled with Tc-99m was using procedures provided in package inserts. In each preparation any unbound Tc-99m was eliminated by Centricon-30 (Amicon) molecular filtration technique and analyzed by ITLC and HPLC. In each of the five preparations, native (except BW 250/183), reduced or conjugated, and radiolabeled proteins were loaded on 4-20% gradient gels under non-reduced or DTT reduced conditions along with M.W. standards.

Electrophoresis was performed for 45 minutes at 160 V using tris glycine buffer at pH 7.3. Gels were then autoradiographed, stained, read with a densitometer and cut and counted for radioactivity in each band.

All preparations had greater than 95% radioactivity associated with proteins and less than 5% colloid. Results of SDS-PAGE analysis under non-reduced and reduced conditions for the three direct and two BFCA preparations are given in Table-I and II respectively. Table-I indicates that both BFCA methods had some but minimal fragmentation with 2-ME the most and AA the least. When digested with DTT, all preparations were fragmented to 50 kD and 25 kD M.W. and the major proportion of the radioactivity was associated with them.

Results indicate that during labeling of MAbs with Tc-99m by both direct and indirect methods, probably some of the disulfide bridges are cleaved and a mixture of intact and fragmented antibodies is produced. These may not only alter tissue distribution but in certain cases may also affect immunoreactivity of labeled protein. A systematic study of each method may therefore be necessary. Nevertheless, direct methods remain simple, reliable and even allow investigators to label MAbs with Re-186 for therapeutic application(10). Further work continues in our laboratory in comparing several other properties of Tc-99m MAbs prepared by the AA and BFCA methods.

Work was supported by NIH CA-R01 57960 to MLT.

REFERENCES

1. Rhodes BA, Zamora PA, Newell KD, et al. Tc-99m labeling of murine antibody fragments. *G. Nucl. Med.* 1986; **27**: 685-91.
2. Schwartz A and Steinstrabber A. A novel approach to Tc-99m labeled monoclonal antibodies. *J. Nucl. Med.* 1987; **28**: 721.
3. Mather SJ and Ellison D. Reduction mediated Tc-99m labeling of monoclonal antibodies. *J. Nucl. Med.* 1990; **31**: 682.
4. Fritzberg AR, Abrams PG, Vanderheyden J-L, et al. Specific and stable labeling of antibodies with Tc-99m with a diamide dithiolate chelating agent. *Pro.Natl. Acad. Sci.* 1985; **85**: 4025-4030.
5. Baidoo KE, Scheffel U and Lever SZ. Tc-99m labeling of proteins: diamino dithio bifunctional chelating agent. *Cancer Res.* 1990; **50**: 799-803.
6. Hnatowich DJ, Mardirosi G, Rusckowski M, Forgrasi M, et al. Direct and indirect labeled antibodies. A comparison of in vitro and animal in vivo properties. *J. Nucl.Med.* 1993; **34**: 109-119.
7. Axworthy DB, Su DB, Fritzberg AR. Comparison of Tc-99m: Direct vs.  $N_2S_4$  chelate labeled NR LU-10 FAb in tumored nude mice. *J. Nucl.Med.* 1992; **33**: 909 (Abstract).
8. Thakur ML, Richard MD, White FW. Monoclonal antibodies as agents for selective radiolabeling of human neutrophils. *J.Nucl. Med.* 1988; **29**: 1814-17
9. Najafi A, Alauddin MA, Siegel ME and Epstein AL. Synthesis and preliminary evaluation of a new chelate  $N_2S_4$  for use in labeling proteins with metallic radionuclides. *Nucl.Med.Biol.* 1991; **18**: 179-85.
10. John E, Thakur ML, DeFulvio JD, et al. Rhenium-186 labeled monoclonal antibodies for radioimmunotherapy: Preparation and evaluation. *J.Nucl.Med.* 1993; **34**: 260-267.

**Table I**

% Protein concentration corresponding to apparent M.W. (kD), before (Pb) and after (Pa) radiolabeling, and % Radioactivity (R) associated with each band (non-reduced).

Agent	150 kD	100 kD	92 kD	50 kD	25 kD
HlgG (Pb)	87.9	6.1	---	1	4.1
(Pa)	---	---	---	---	---
(R)	---	---	---	---	---
AA (Pb)	81.9	5.8	---	6.3	6.1
(Pa)	46.4	10.8	---	14.1	28.5
(R)	70.9	8.2	---	6.5	14.5
SnCl <sub>2</sub> (Pb)	24.5	---	1.2	45.1	20.6
(Pa)	21.9	14.8	13.8	34.3	16.2
(R)	47.8	8.8	8.4	24.6	10.5
2-ME (Pb)	10.3	---	---	45	51.2
(Pa)	3.9	---	---	45	51.2
(R)	17	---	---	49.4	32.7
C-DTPA (Pb)	71.5	7.7	---	20.8	---
(Pa)	61	11.9	---	9	7.3
(R)	79.8	5	---	10.9	50
N <sub>2</sub> S <sub>4</sub> (Pb)	91.9	8.1	---	---	---
(Pa)	65	15	---	7.3	13
(R)	72	16.1	---	11.7	---

**Table II**

% Protein concentration corresponding to apparent M.W. (kD) before (Pb) and after (Pa) radiolabeling and % radioactivity (R) associated with each band (DTT reduced).

Agent	150kD	100kD	50kD	25kD
HlgG (Pb)	---	8.5	61.7	29.8
(Pa)	---	---	---	---
(R)	---	---	---	---
AA (Pb)	---	10.3	50.6	39.1
(Pa)	---	9.3	28.4	62.3
(R)	---	18	36	46
SnCl <sub>2</sub> (Pb)	---	4.7	60.6	34.7
(Pa)	---	15.6	23.9	60.5
(R)	---	7.9	50	42.1
2-ME (Pb)	---	---	50.6	49.4
(Pa)	---	---	38.1	61.9
(R)	---	---	72	28
C-DTPA (Pb)	---	17.2	41.7	41.1
(Pa)	---	7.9	43.1	49
(R)	---	16	45	39
N <sub>2</sub> S <sub>4</sub> (Pb)	---	22.7	53.7	23.6
(Pa)	---	11.7	63.3	25
(R)	---	11.3	51.6	36.7

**Tc-99m labeled monoclonal antibodies for imaging tumors:  
Influence of biological response modifiers**

Li, J.<sup>1</sup> Merton, D. A.<sup>2</sup> Barr, J.<sup>1</sup> Wilder, S.<sup>1</sup> Barravecchio, D.<sup>2</sup> Goldberg, B.<sup>2</sup>  
and Thakur, M. L.<sup>1</sup>

Depts. of Radiation Oncology and Nuclear Medicine (1), and Radiology (2), Thomas Jefferson University, Philadelphia, PA 19107.

Previously we have shown that when certain biological response modifiers (BRMs) are given to tumor bearing animals, prior to the administration of radiolabeled monoclonal antibodies (MAbs), there is a significant enhancement in the tumor uptake of radioactivity (1). This investigation was designed to validate the hypothesis that following the administration of these cytokines there is a transient increase in temperature and blood flow that may in part result in increased capillary permeability and extracellular fluid volume, thereby augmenting the tumor uptake of radioactivity associated with MAbs.

Human melanoma tumors were grown in a thigh of nude mice by subcutaneous and intramuscular implantation of approximately  $5 \times 10^6$  WM-9 cells grown in cell culture. In order to maintain the body temperature following anesthesia, animals were placed on a mat with circulating water at 37°C and covered with a sheet of gauze.

Two thermocouple (25 G needle) probes, one into a tumor and the other into the contralateral thigh, were inserted and temperatures were recorded every 5 minutes for 20 minutes prior to and for 90 minutes after the i.m. injection of BRMs and saline as control.

Blood flow, before and after administration of the agents, was monitored by laser Doppler perfusion monitor (LDPM, Perimed, NJ) and a separate group of mice also by a high resolution, color Doppler ultrasound imaging (CDI, Diasonics, CA) system. In LDPM (2 mW, He-Ne laser, 632.8 um wavelength), surface probe was used and blood flow was monitored continuously using a chart recorder. In CDI, 10 MHz flat linear array transducer was used. CDI was performed with acoustic coupling gel placed over the tumor and normal thigh. CDI allowed localization of a single tumor vessel from which continuous spectral Doppler flow signals were obtained over the duration of each experiment. Peak systolic (PS) and end diastolic (ED) amplitudes (KHz) were measured using onboard calipers and from these resistive indices (RI), using the formula  $RI = (PS - ED) / PS$  were calculated.

Human recombinant interferon-alpha-2b (IFN) known to inhibit growth of both normal and tumor cells and stimulate immune effector cell function was chosen as a model BRM (2).

Results showed that the 15 -20 minutes following i.m. administration of 20K IU IFN, there was a modest increase in tumor temperature. However, the general decrease in body temperature following and during anesthesia made these measurements inconsistent and did not permit us to draw a definite conclusion.

LDPM showed 20-30% increase in tumor blood flow perfusion units approximately 30 minutes after the administration of IFN and was persistent for longer than 30 minutes. This increase following saline injection was only 0-5%. (Fig.1)

A response consistent with the LDPM was also observed with CDI. Approximately 30 minutes post injection of IFN, the tumor blood flow signals were



visibly increased in intensity, with a significant increase in PS and ED ( 1 KHz vs. 2.5 KHz and 0.5 KHz vs. 1.5 KHz respectively) amplitudes. (Fig.2, middle panel) No significant increase in cardiac rate was observed. (Fig.2, top panel)

200 ug of angiotensin-II, a potent vasoconstrictor peptide was injected i.v. Angiotensin-II can increase peripheral resistance mainly in cutaneous, splanchnic and renal blood vessels, both directly and via the sympathetic nervous system.(2) Immediate enhancement of tumor blood flow was recorded as evidenced by the characteristic increase in PS and ED amplitudes (0.4 KHz vs. 1.5 KHz and 0.2 KHz vs. 0.5 KHz) as well as in cardiac rate (180/min. vs. 300/min.) (Fig.2, lower panel)

Enhanced perfusion changes in the normal thigh with i.m. administration of IFN and with i.v. administration of angiotensin-II were also observed by both LDPM and CDI techniques. However, these changes lasted for less than 10 minutes.

In summary, our results show that i) BRMs enhance tumor blood perfusion which last for a much longer period of time than that in the normal tissue and that ii) LDPM and CDI provide excellent means of measuring tumor perfusion changes, even in small living animals such as the mice where radioactive tracers cannot be easily used for perfusion measurement.

Work was supported by DOE FG02-92 ER 61485 to MLT.

#### References

- 1). M.L.Thakur and J.D.DeFulvio. *J. Immunol. Methods.* 137, 217-224, 1991.
- 2). B.E.Nelson and E.C.Borden. *Seminars in Surg. Onco.* 5, 391-401, 1989.
- 3). M.J.Trotter, et al. *Eur. J. Cancer,* 27, 887-893, 1991.

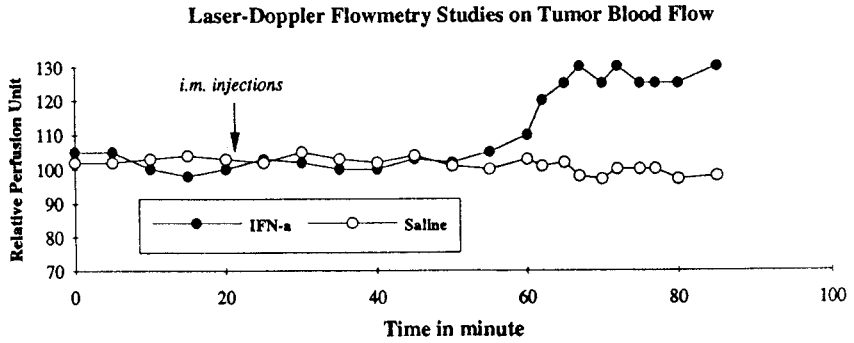


Fig. 1: Continuous laser Doppler perfusion measurement profile 20 minutes before and 90 minute after the i.m. administration of 20K IU of IFN. Perfusion units are arbitrary and were derived from the chart recorder.

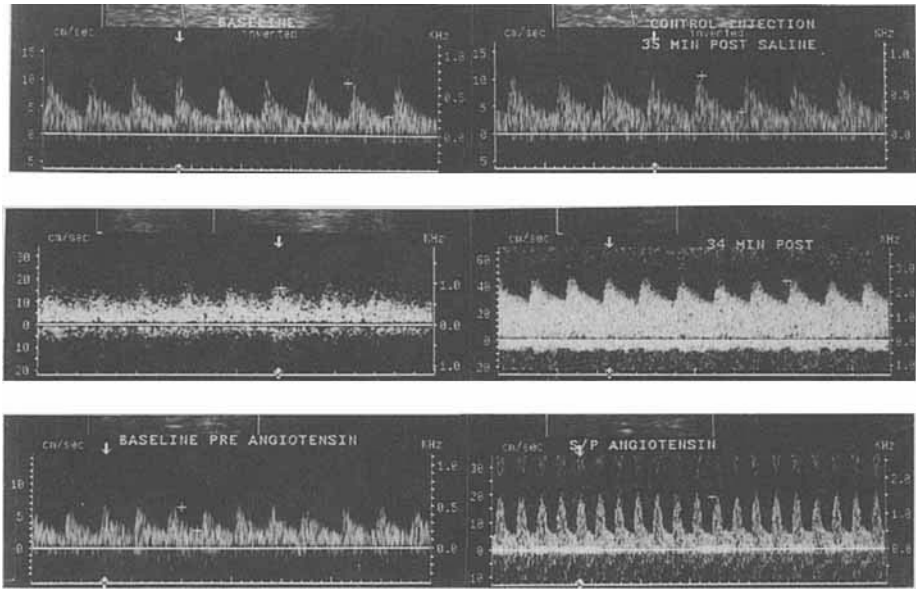


Fig. 2: A composite of 6 CDI images of tumor perfusion prior to (left) and after (right) administration of saline (control, top panel), 20K IU IFN (i.m., middle panel) and 200 µg of angiotensin-II (i.v., bottom panel). PS and ED are recorded at various points along cardiac cycle.

**Antithrombospondin Monoclonal Antibody for Visualization of Thrombi**  
MITKEVICH O.V., SAMOKHIN G.P., PETROV A.D., TORCHILIN V.P.,  
MARTIANOV B.M., EGOROVA E.F., SERGIENKO V.B., MALOV A.G.,  
KUZNETSOVA E.V., ZHDANOVICH M.U. Cardiology Research Center,  
Academy of Medical Science, Moscow, Russia

Significant difficulties remain in defining the precise anatomic location and extent of the thrombus, especially in the entire venous system (1,2). In recent years several monoclonal antibodies (MAb) against different components of thrombi have been proposed as site-specific radiopharmaceuticals for clot detection. These are MAbs against different sites of fibrin which do not react with fibrinogen (3,4) and MAbs against some platelets membrane proteins (5,6). In our work we have used a MAb against human thrombospondin (TS).

TS is a glycoprotein with molecular mass 420 kD. It is located mainly in platelet alpha-granules and in extracellular matrix (7). In normal TS is not exposed into the blood circulation and its concentration in plasma is about 100 ng/ml (8). During clot formation accompanied by platelets activation TS is secreted from alpha-granules, binds to platelets surface and fibrin and incorporates with them into the thrombi (7). Therefore TS may be a target for the radioactively labeled MAb for thrombi imaging.

We have obtained MAb 4C1 against TS. This MAb was not inhibited by the plasma components fibrinogen and fibronectin and by heparin present in plasma during thrombolytic therapy, which are known to bind to TS. We have shown *in vitro*, that MAB 4C1 binds to human and rabbit clots. The binding of 4C1 MAb to clots was 8-10

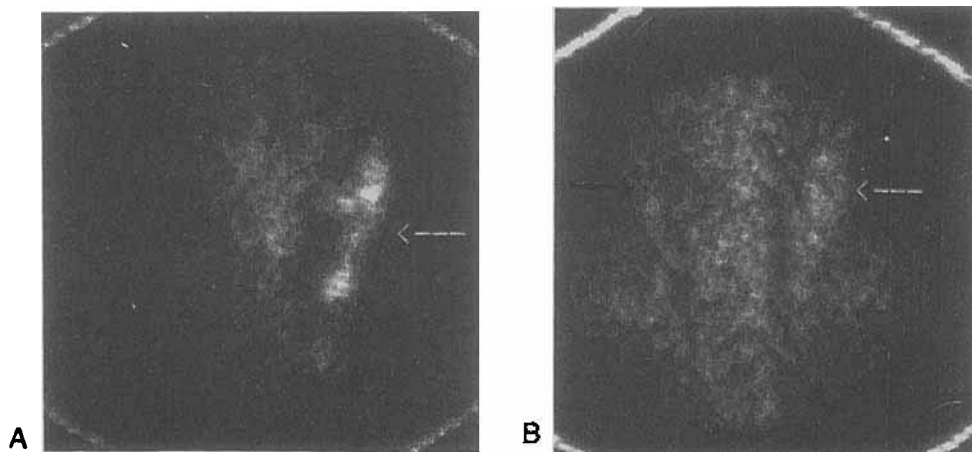


Figure 1. Gamma camera images of rabbit thrombi in left v. jugularis (indicated by arrow) at 24 hour postinjection. A: imaging by  $^{99m}\text{Tc}$  labeled MAb 4C1, C: imaging by  $^{99m}\text{Tc}$  labeled MAb 5A2.

fold higher than that of nonspecific immunoglobulin. The binding of 4C1 MAb with Ts was only two-fold inhibited by rabbit plasma. This allows to perform the experiments *in vivo*.

We used as *in vivo* experimental model the artificial thrombi, made in vein jugularis of rabbit. The artificial thrombi was made by injection of suspension of 1000 mg of magnetic particles into left rabbit ear, while holding a magnet in place over the left v. jugularis. Four hours later the magnet was taken off and the formation and location of the thrombi was confirmed by an X-ray study. After that 100  $\mu\text{g}$  of 4C1 MAb labeled by  $^{99\text{m}}\text{Tc}$  (2-3 MCi) was injected into the opposite ear.

Thrombi was successfully visualized at 24h postinjection using a gamma camera (fig. 1). As the control we used the MAb 5A2 against the C-terminal part of A $\alpha$ -chain of fibrinogen which is easily released during plasmin digestion and is not present in sufficient quantity in the thrombi. Ratios of radioactivity in thrombi to radioactivity in blood were calculated from direct counts at 24 hours after injection in 8 rabbits and were found to be  $3,89 \pm 0,9$  (M $\pm$ SEM). We have studied the blood clearance of 4C1 MAb (fig.2). Blood samples (0,5-1,0  $\mu\text{l}$ ) were obtained from 8 rabbits weighted and then counted in a gamma scintillation counter. The half-life in the blood of 4C1 MAb was approximately 45 min, which is better than for some antibodies or their fragments (4, 9,10).

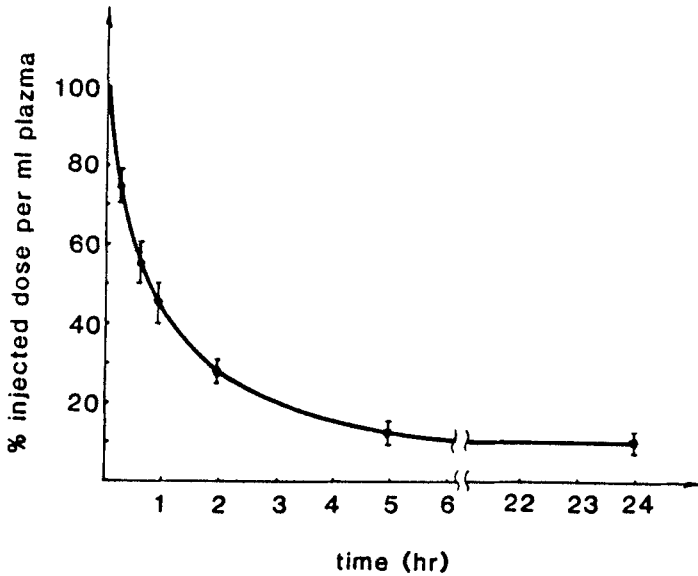


Figure 2. Plasma disappearance of  $^{99\text{m}}\text{Tc}$ -labeled 4C1 MAb.

Thus MAb against TS accumulates into the thrombi despite a low concentration there of TS. The half-life of studied MAb is sufficiently short to get a good image on gamma-camera and to make clinical potential. We conclude that the MAb against TS may be used for radiovisualization of thrombi.

1. Ezekowitz M.D., Pope Ch.F., Sostman H.D., Smith E.O., Glickman M., Rapoport St., Sniderman K.W., Friedlaender G., Pelker R.R., Taylor F.B., Zaret B.L. - *Circulation* 73: 668(1986).
2. Knight L.C. - *J.Nucl. Med.* 32: 791(1991).
3. Faucal Ph.D., Peltier P., Planchon B., Dupas B., Touze M.-D., Baron D., Scaible T., Berger H.J., Chatal J.-Fr. - *J. Nucl. Med.* 32: 785(1991).
4. Walker K.Z., Chafagi F., Bautovich G.J., Boniface G.R., Bundeser P.G., Rylatt D.B. - *Thromb. Res.* 52: 269(1988).
5. Palabrica Th.M., Furie B.C., Konstam M.A., Aronovitz M.J., Connolly R., Brockway B.A., Raberg K.L., Furie B. - *Proc. Natl. Acad.Sci. USA* 86: 1036(1989).
6. Som P., Oster Z.H., Zamora P.O., Yamamoto K., Sacker D.F., Brill A.B., Newell K.D., Rhodes B.A. - *J.Nucl.Med.* 27: 1315(1986).
7. Majack R.A. and Bornstein P. - *Cell Membranes* 3: 55(1987).
8. Bale M.D. and Moshen D.F. - *J. Biol. Chem.* 261: 862(1986).
9. Knight L.c., Maures A.H., Ammar I.A., Shealy D.J., Mattis J.A. - *J.Nucl. Med.* 29: 494(1988).
10. Hashimoto Y., Stassen J.M., Leclef B., De Roo M., Vendeerays A., Melin J., Verhoeven-Mester D., Trouet A., Collen D. - *Radiology* 171: 223(1989).

**$^{99m}\text{Tc}$  LABELED AUTOLOGOUS ALBUMIN: A POTENTIAL AGENT FOR THE DETECTION OF PROTEIN LOSING ENTEROPATHY (PLE).**

AMARTEY J.K\* and RIFAI A . Division of Nuclear Medicine, King Faisal Specialist Hospital and Research Centre, Box 3354, Riyadh 11211, Kingdom of Saudi Arabia.

Recently we reported a method for labeling peptides and proteins with technetium using a 2-iminothiolane (2-IT) derivative (1,3). This technique has been applied to the labeling of autologous albumin from rats, rabbits and human. This radiolabeled material has been evaluated in animals aimed at assessing its possible application in the imaging of PLE, a condition characterized by the secretion of serum albumin into the gastrointestinal tract (2).

Serum proteins were isolated from 5 ml whole blood after clotting at room temperature for approximately 30 min. The clot was compressed by centrifugation at 1500 rpm for 5 min. The serum (0.5 ml) was pipetted and 1 mg of 2-IT.HCl added. The mixture was allowed to react for 90 min. The radiolabeling procedure was as previously described (3). Typically, 1110-2220 MBq (30-60 mCi) of fresh pertechnetate eluate was added to the derivatized and pre-tinned protein, and allowed to incubate for 30 min. Aliquots were taken for analysis on ITLC-SG and by HPLC.

HPLC (size exclusion column) analysis of the isolated serum proteins consistently showed a major peak with the same retention time as authentic albumin. There was a preceding shoulder peak which was presumed to be immunoglobulins. This technique consistently gave very high labeling efficiency (>95%) as determined by ITLC and HPLC, and a typical analysis is shown in figure 1. The biodistribution in normal rats showed that the radiolabeled material remained in the circulation. A very low level of activity was present in the liver (Table 1). Scintigraphic images of a rabbit confirmed this observation (figure 2). The duration of the procedure was approximately 2.5 h. This time was comparable to the classical WBC labeling protocol. The biodistribution and imaging results indicated that the radiopharmaceutical remained in the circulation, with a very small fraction being excreted through the feces. The results clearly showed that  $^{99m}\text{Tc}$  labeled autologous serum proteins may be valuable in the detection of PLE. The procedure can be performed in a manner similar to the classical cell labeling procedure for infection detection. The potential application of this technique demand further studies.

## References.

1. Jue R., Lambert J.M., Pierce L.R., et al. *Biochemistry* 17: 5399 (1978).
2. Kowalsky R.J and Perry R.J. *Radiopharmaceuticals in Nuclear Medicine Practice* p. 451. Appleton & Lange, Norwalk, 1987.
3. Amartey J.K. *Nucl. Med. Biol.* (1993) In Press.

Table 1: Biodistribution of  $^{99m}\text{Tc}$  labeled autologous albumin in normal rats. The values are mean and standard deviation of % injected dose per gram (n=5).

Tissue	Time(h)	
	4	24
Blood	0.58+/-0.36	0.13+/-0.01
Liver	1.77+/-0.15	0.46+/-0.37
Kidneys	8.63+/-2.88	5.73+/-0.32
Intestine	0.31+/-0.24	0.05+/-0.02
Feces	-----	0.59

Figure 1. The HPLC analysis of the reaction mixture on size exclusion column. Eluent was water at 1.0 ml/min. The labeled albumin eluted at  $R_t = 5.8$  min, and free pertechnetate at  $R_t = 12.1$  min. The UV absorbance at 254nm is shown for comparison.

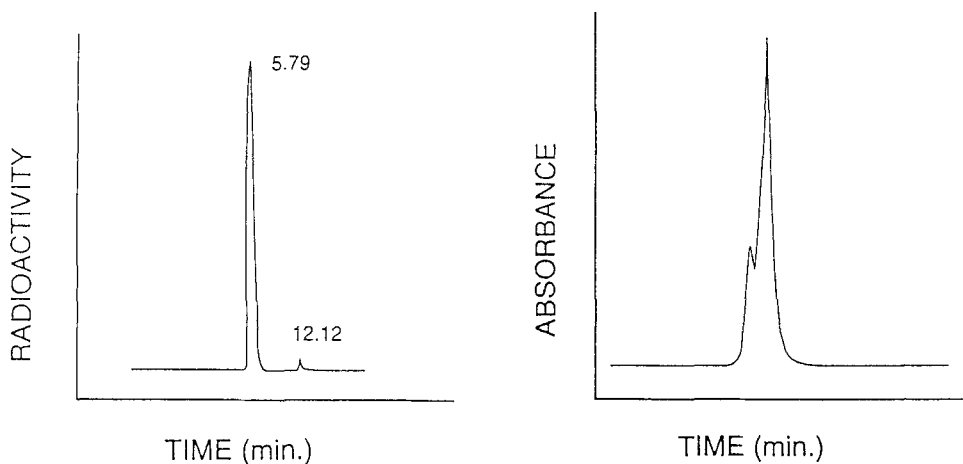
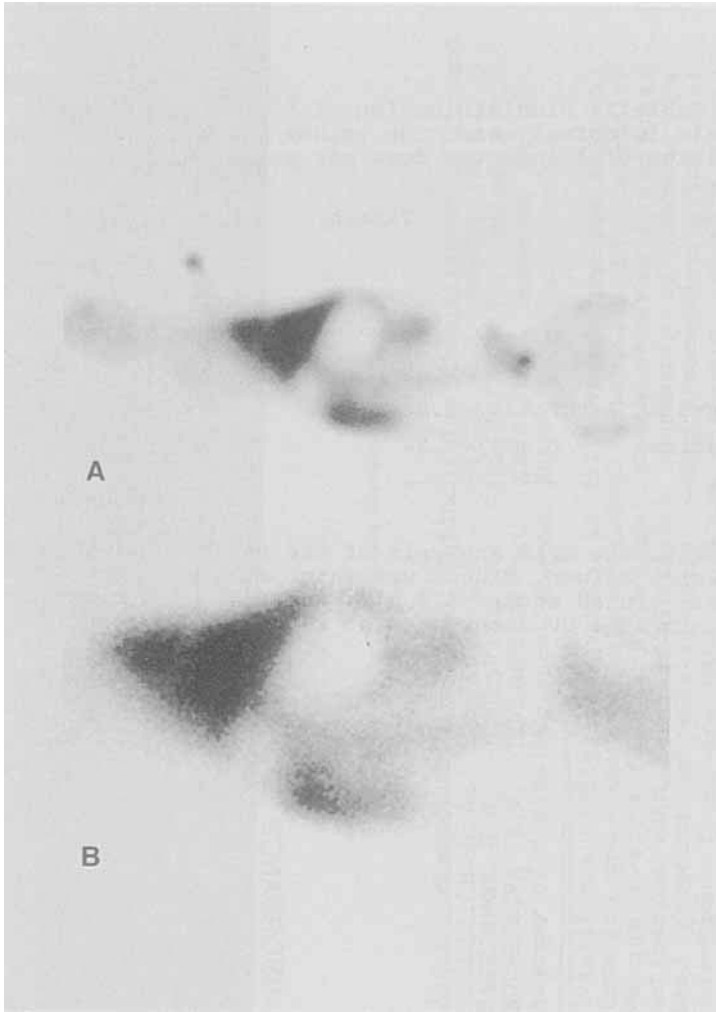


Figure 2. Delayed (A) and blood pool (B) images of a rabbit injected with 37 MBq of the radiopharmaceutical. The radioactivity clearly localized in well vascularized organs such as the heart, lungs, liver, kidneys and spleen.





Radiosilver - A Candidate Radionuclide for Radioimmunotherapy :  
Linkage to IgG. Hazra D.K., Lahiri, V.L.; Painuly, N.K.,  
Gupta, A.K.; Gupta, R.K.; Pathak, M.; Khanna, P.; Khanna, Padma  
and Saran, S.: Nuclear Medicine & RIA Unit, Postgraduate Department  
of Medicine, S.N. Medical College, Agra-282 003 (INDIA)

Various radionuclides are currently under investigation in the West as possible warheads for radioimmunotherapy, notably  $I^{131}$  and  $Y^{90}$ . This choice of radionuclide for radioimmunotherapy depends inter alia on (1) desired physical characteristics of the radioisotopes viz. half life, photon energy, (2) chemical reactions involved for incorporating the radionuclide into the antibody, (3) appropriate biocompatibility of the selected radionuclides, (4) Daughter/parents/contaminant isotopes as well as (5) all the reagents contained in the material being injected in-vivo, (6) bio-distribution and in-vitro and in-vivo stability of radionuclide-antibody linkage, i.e. lack of transchelation and the resistance of the radionuclide antibody combination to biodegradation e.g. dehalogenases.

$I^{131}$  poses problems, because of its energetic gamma as well as dehalogenation leading to nontarget irradiation.  $Y^{90}$  is a bone seeker and in case the isotope dissociates from the radionuclide-antibody complex, this can lead to unacceptable irradiation of bone. This is specially important if the host mounts a human anti-mouse antibody (HAMA) reaction.

We, therefore, considered the beta emitters  $_{47}Ag^{111}$  ( $T_{1/2}$  = 7.45 days) and  $_{79}Au^{199}$  ( $T_{1/2}$  = 3.15 days) to be suitable in our conditions for evaluation. Since silver is monovalent, it is difficult to link to conventional bifunctional chelates. We, therefore, explored the use of sulphur based linkage (Hazra et al. 1991). Encouraged by Thakur and DeFulvio technique (1990) of linking

technetium to disulphide groups in antibodies reduced by ascorbic acid which is eminently biocompatible, we assessed the linkage using  $^{47}\text{Ag}^{110\text{m}}$  as radio tracer.

1 mg immunoglobulin was reduced with 3 mg of ascorbic acid, this corresponded to a molar excess of ascorbic acid 3/176:1/200000,  $1:2.93 \times 10^{-4}$  dissolved in 500 ul of distilled water. This was reacted with  $\text{Ag}^{110\text{m}}$  (1mCi) in a volume of 1 ml corresponding for a ratio of 1 atom of radiosilver/molecule of immunoglobulin. The reaction product was submitted to column chromatography on a PD-10 Sephadex column as well as paper chromatography. It appears that there is significant binding of the radiosilver with the reduced immunoglobulins (Fig. 1; Fig. 2), but the nature of binding remains moot as NMR studies to further characterisation of binding are awaited.

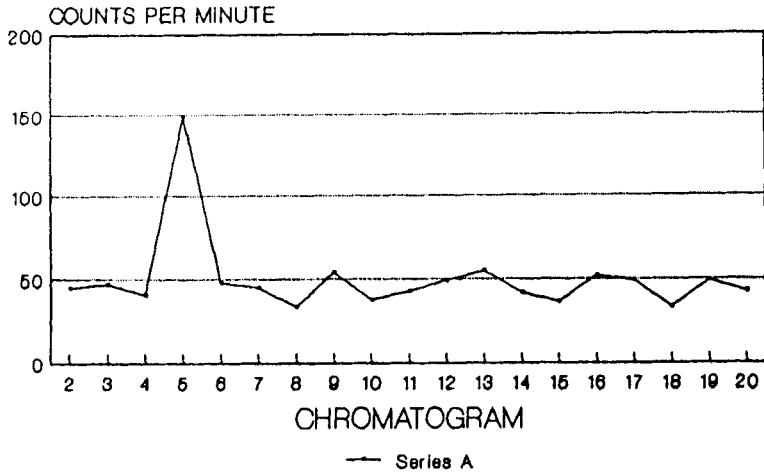
Further in-vitro and in-vivo stability of the Ag + IgG complex under physiological conditions needs to be examined. Biodistribution studies are also planned.

Acknowledgements: This work was supported by DST and ICMR, Government of India Research Projects.

References:

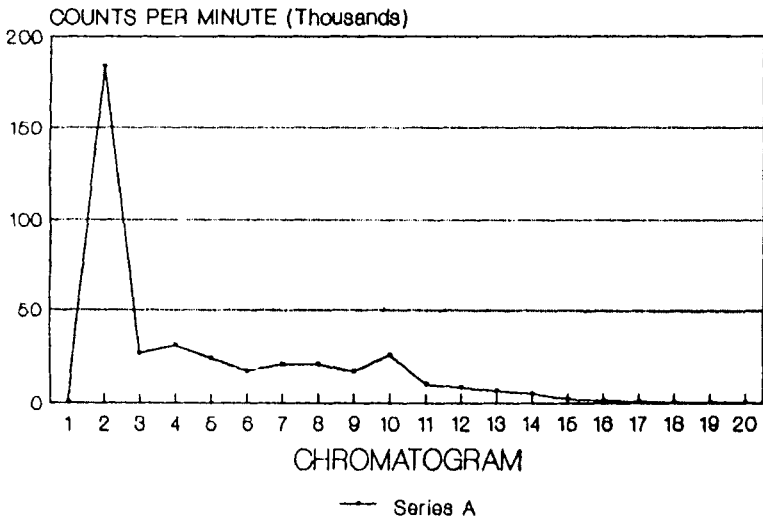
1. Hazra DK, Chaturvedi GK, et al. (1991) Role of Alcoholic Solvents in Silver Complexation, 8th International Hammersmith Symposium Greece, May 7-12.
2. Thakur ML, DeFulvio JD (1990). *Biotechniques* 8: 512-516.

FIG-1 PD-10 CHROMATOGRAPHY  
OF Ag-110m WITH REDUCED IgG



EACH FRACTION IS 2 DROPS i.e. 50ul  
COLUMN WAS PREEQUILIBRATED WITH 1% BSA

FIG-2 RADIO-CHROMATOGRAPHY  
COMPLEX FORMED BY Ag-110m+ REDUCED IgG

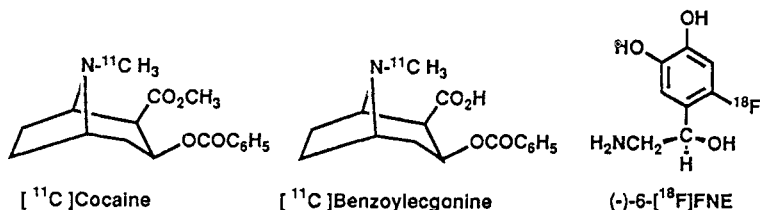


**Pharmacokinetics of [<sup>11</sup>C]Cocaine and [<sup>11</sup>C]Benzoylecgonine in Baboon Heart and the Effect of Cocaine Treatment on the Myocardial Norepinephrine Transporter**

J. S. Fowler, Y-S. Ding, N. D. Volkow, T. Martin, R. R. MacGregor, S. Dewey, P. King, N. Pappas, C. Shea, S. J. Gatley, D. Schlyer, J. Logan and A. P. Wolf, Brookhaven National Laboratory, Upton, New York 11973

Cardiotoxicity is a major medical complication in cocaine abuse. Cocaine has two major pharmacological properties affecting the cardiovascular system: its ability to block the reuptake of norepinephrine (NE) thereby disabling the major mechanism by which the heart terminates sympathetic neuronal activity and local anesthetic effects, reducing sodium transport and increasing the threshold for an action potential. (1) PET studies with [<sup>11</sup>C]cocaine have shown that there is rapid significant uptake of cocaine in the human heart. (2) A recent study by Melon, et al has shown that an acute dose of cocaine inhibits the uptake of [<sup>11</sup>C]hydroxyephedrine, a tracer for the cardiac sympathetic neuron. (3) Though a high uptake of cocaine is observed in the human heart with PET, its residence time in the heart is shorter than the observed chronotropic effects of cocaine (ca. 45 minutes) raising questions as to the mechanisms involved. (4) Additionally, persistent left ventricular dysfunction after cocaine treatment has been observed in rabbits *in vivo* but not *in vitro*. (5)

We report the results of a multi-tracer study to examine the pharmacokinetics and pharmacodynamics cocaine in baboon heart. We used [<sup>11</sup>C]cocaine to examine the pharmacological profile of cocaine binding and (-)-6-[<sup>18</sup>F]fluoronorepinephrine ((-)-6[<sup>18</sup>F]NE) (6) to examine the time course of the effects of cocaine on the norepinephrine transporter. We also synthesized [<sup>11</sup>C]benzoylecgonine, a metabolite of cocaine which is a potent vasoconstrictor (7) and examined its behavior in baboon heart.



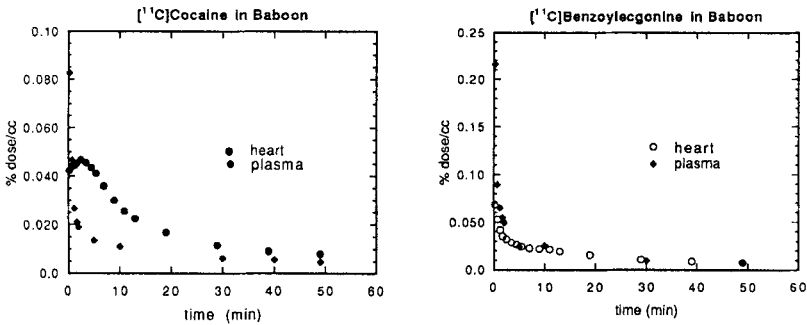
Serial studies with [<sup>11</sup>C]cocaine were performed two hours apart on five different baboons as described previously (8) with the following interventions prior to the second [<sup>11</sup>C]cocaine injection: (1) desipramine (0.5 mg/kg 30 min prior); (2) tomoxetine, a highly specific inhibitor of the norepinephrine transporter (2 mg/kg, 30 min prior) and (3) cocaine (2 mg/kg, 2 min prior); (4) nomifensine (2 mg/kg; 30 min prior); cogentin (0.1 mg/kg; 60 min prior). Arterial input functions were measured for each study.

[<sup>11</sup>C]Benzoylecgonine was synthesized from nor-benzoylecgonine and [<sup>11</sup>C]methyl iodide. The myocardial uptake and retention of [<sup>11</sup>C]benzoylecgonine in baboon was compared with that of [<sup>11</sup>C]cocaine.

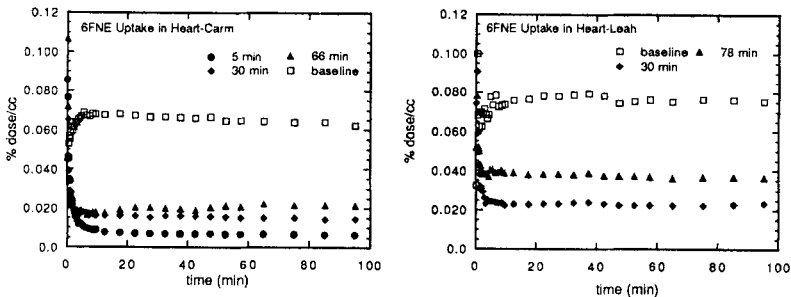
Two different baboons received baseline studies with (-)-6[<sup>18</sup>F]NE as described previously. (6) In one of the baboons, three additional (-)-6[<sup>18</sup>F]NE studies were

carried out with a 9-14 day interval between each study. For these three studies, cocaine (2 mg/kg) was administered at 5 minutes, 30 minutes, or 66 minutes prior to the (-)-6[<sup>18</sup>F]NE. In the second baboon, cocaine (2 mg/kg) was administered at 30 minutes, and 78 minutes prior to the (-)-6[<sup>18</sup>F]NE. Arterial input functions were measured for each study as described previously.

In each of the baseline studies, cocaine uptake in the heart peaked rapidly, reaching a maximum value at 1-2.5 minutes and then decreasing rapidly with a clearance half time from peak uptake that ranged from 4-9 minutes. Peak uptake ranged from 0.036-0.055% dose/gram. By 30 minutes, carbon-11 in heart had cleared to 13 to 24% of peak value. None of the drugs inhibited [<sup>11</sup>C]cocaine uptake in heart. Values of the integrated plasma input functions at 5 and 30 minutes correlated with the integrated heart uptake at 5 and 30 minutes and accounted for variability in peak uptake and clearance time in different baboons. Cocaine pretreatment resulted in a *slower* clearance ( $t_{1/2}$  (cocaine): 12.3 min vs 9 min (baseline) and a significantly (50%) larger plasma input function. [<sup>11</sup>C]benzoylcegonine showed negligible uptake and retention in myocardium. Time-activity curves for heart and plasma for [<sup>11</sup>C]cocaine and [<sup>11</sup>C]benzoylcegonine for the same baboon are shown below.



Studies with (-)-6[<sup>18</sup>F]NE at baseline revealed the characteristic pattern of high uptake into the heart which peaks rapidly after injection and plateaus thereafter. Cocaine reduced (-)-6[<sup>18</sup>F]NE uptake into the myocardium to 10 % of the baseline value. The magnitude of blockade when cocaine (i.v.) was administered 5 minutes before (-)-6[<sup>18</sup>F]NE was similar to that reported previously with pretreatment with desipramine.(6) The effect was prolonged with 29 % and 48 % of baseline uptake being recovered by 66 and 78 minutes. Time-activity curves for (-)-6[<sup>18</sup>F]NE for the two baboons at different times after cocaine administration are shown below.



As was observed previously in human studies, there was significant accumulation of [<sup>11</sup>C]cocaine in baboon heart. We were unable to inhibit cocaine uptake by cocaine or by inhibitors of the norepinephrine transporter (desipramine and tomoxetine), the dopamine transporter (nomifensine) or cholinergic receptors (benztropine). However, even though we were unable to document binding of cocaine into the norepinephrine transporter as assessed by the inability of desipramine or tomoxetine to block its uptake, we were able to demonstrate inhibition of the function of the norepinephrine transporter by cocaine as reflected by the blockade of (-)-6[<sup>18</sup>F]NE uptake. While this apparent discrepancy could reflect a different binding site for desipramine and tomoxetine and cocaine at the norepinephrine transporter (for a discussion see 9), the time course of cocaine's inhibition of the NE transporter as demonstrated in this study using (-)-6[<sup>18</sup>F]NE argues against a direct effect of cocaine mediated by its presence in myocardial tissue. Possible mechanisms for cocaine's inhibition of the norepinephrine transporter include (1) cocaine promoted release of catecholamines from the adrenals which might compete with uptake of (-)-6[<sup>18</sup>F]NE. (10,11); (2) cocaine promoted alteration of the concentration and binding properties of the norepinephrine transporter; (3) myocardial stunning due to brief ischemia produced by cocaine (5). Although we examined the uptake of [<sup>11</sup>C]benzoylcegonine in heart because of its known vasoactive properties, its lack of uptake and retention argue against a direct effect in mediating cardiovascular effects of cocaine.

In summary, the pharmacokinetics and pharmacological profile of [<sup>11</sup>C]cocaine as measured in this study do not completely account for its effects on the norepinephrine transporter. However, since cocaine has been shown to increase circulating catecholamines which will interact with myocardial cells in which the protective mechanisms for catecholamine removal by the transporter have been inhibited, the marked inhibition of the norepinephrine transporter could enhance the cardiotoxic properties of cocaine. Our results indicate that the effects of cocaine on the NE transporter have a significantly longer duration than either the subjective or the measured cardiovascular effects. A decreased transporter function in the absence of observable physiological symptoms, could put the cocaine abuser who repeatedly uses the drug at risk for cardiovascular complications. It is also interesting that 2 mg of cocaine almost totally inhibited the uptake of (-)-6[<sup>18</sup>F]NE to an extent equivalent to that observed with desipramine. (6) This is of relevance also for its therapeutic implications since desipramine is one of the pharmacological treatment given to cocaine abusers. Possible synergistic interactions between these two drugs with respect to their cardiotoxic effects should be evaluated.

Supported by DOE/OHER; NIH (NINDS); NIDA.

- (1) R. A. Kloner, et al, *Circulation* 85:407-419, 1992.
- (2) N. D. Volkow, et al, *J. Nucl. Med. J. Nucl. Med.* 33:521-525, 1992.
- (3) P. G. Melon, et al, *J. Nucl. Med.* 33: 994, 1992.
- (4) R. W. Foltin and M. W. Fischman, *J. Pharm Exp. Ther.* 257: 247-261, 1991.
- (5) C. F. Pilati, et al, *P. S. E. B. M.* 203: 100-107, 1993.
- (6) Y-S. Ding, et al, *J. Nucl. Med.* 34: 619-629, 1993.
- (7) J. A. Madden and R. H. Powers, *Life Sci*, 47: 1109-1114, 1990.
- (8) J. S. Fowler, et al, *Synapse* 4: 371-377, 1989.
- (9) P. M. Laduron, *Biochem. Pharmacol.* 33: 833-839, 1984.
- (10) C.C. Chiueh and I. Kopin, *J. Pharm. Exp. Ther.* 205: 148-154, 1978.
- (11) G. Nahas, et al, *Cocaine and the Sympathoadrenal System*, in *Adv. in Bioscience*, Pergamon Press, vol 80: 151-164, 1991.

**Stereoselective Syntheses of R,R-IQNB and Fluoroalkyl Analogs of QNB**

KIESEWETTER, D.O. SILVERTON, J.V.<sup>#</sup>, ECKELMAN, W.C. Positron Emission Tomography Department, CC, and <sup>#</sup>Laboratory of Biophysical Chemistry, NHLBI, National Institutes of Health, 9000 Rockville Pike, Bethesda, MD 20892, U.S.A.

R-Quinuclidinyl-R-iodobenzilate (R,R-IQNB, **22**) has been labeled with <sup>123</sup>I and <sup>125</sup>I as an agent for *in vitro* assays as well as *in vivo* imaging with single photon emission computed tomography<sup>1</sup>. The R configuration at the quinuclidinyl center provides higher anticholinergic activity than does the S as is demonstrated by the higher anticholinergic activity of R-quinuclidinyl benzilate compared to its S enantiomer.<sup>2</sup> Although the absolute configuration at the bis benzilic center of IQNB is uncertain, the configuration has an interesting consequence. The binding affinity of R,R-IQNB for M1 ( $K_a$   $8.93 \pm 1.36 \times 10^9$  M<sup>-1</sup>) is 3 fold higher than its diastereomer, R-quinuclidinyl-S-iodobenzilate (R,S-IQNB), ( $K_a$   $2.90 \pm 0.45 \times 10^9$  M<sup>-1</sup>)<sup>3,4</sup>. However the dissociation rate of R,S-IQNB is 13 times faster from M1<sup>3,4</sup> and 21 times faster from m1<sup>5</sup> than that of R,R-IQNB. The configurational assignment at the bis-benzylic center is based on earlier literature that reported higher muscarinic activity for R-2-substituted-2-hydroxy phenyl acetates<sup>6</sup>.

We have developed a stereoselective synthesis of chiral benzilic acids based on the use of a chiral auxiliary, 8-phenylmenthol<sup>7,8</sup>, which provides R-iodobenzilic acid (Scheme 1). Using this established chiral synthetic method and HPLC analysis of the diastereomers (Figure 1), the previous literature assignment of the absolute configuration was verified. The absolute configuration of a sample of R,R-IQNB, provided by Nordion, was also verified by single crystal X-ray diffraction analysis.

Using the same synthetic methodology, we have prepared R or S fluoroalkyl benzilic acids which are subsequently coupled to R or S quinuclidinol. The *in vitro* binding of these compounds was evaluated by NovaScreen with a five point binding curve. The assays were conducted as follows: M1 -<sup>3</sup>H-pirenzepine, bovine striatal membranes with atropine (10<sup>-9</sup>M) as positive control; M2 -<sup>3</sup>H-AF-DX 384, rat heart membrane with methoctramine as positive control (10<sup>-6</sup>M); M3 -<sup>3</sup>H-N-methylscopolamine, guinea pig ileum with 4-DAMP as the positive control, atropine as displacer. R,S-Fluoropropyl QNB and R,S-fluoroethyl QNB display nearly equivalent binding to M1 and M2. However, R,R-fluoroethyl QNB and R,R,S-fluoropropyl QNB display nearly 9 fold higher M1 affinity than M2. Of the diastereomeric fluoroethyl QNB analogs, the R,S diastereomer shows 3 fold higher affinity at M1 and 20 fold higher affinity at M2 than the R,R diastereomer. In the current cholinergic hypothesis of Alzheimer's disease, the M2 presynaptic receptor appears to decrease. This decrease is related to decreased acetylcholine release. Since the R,S fluoroethyl and R,S fluoropropyl QNB display high affinity for the M2 receptor, they may be useful for determining the decrease in receptor concentration in Alzheimer's disease using positron emission tomography.

## REFERENCES

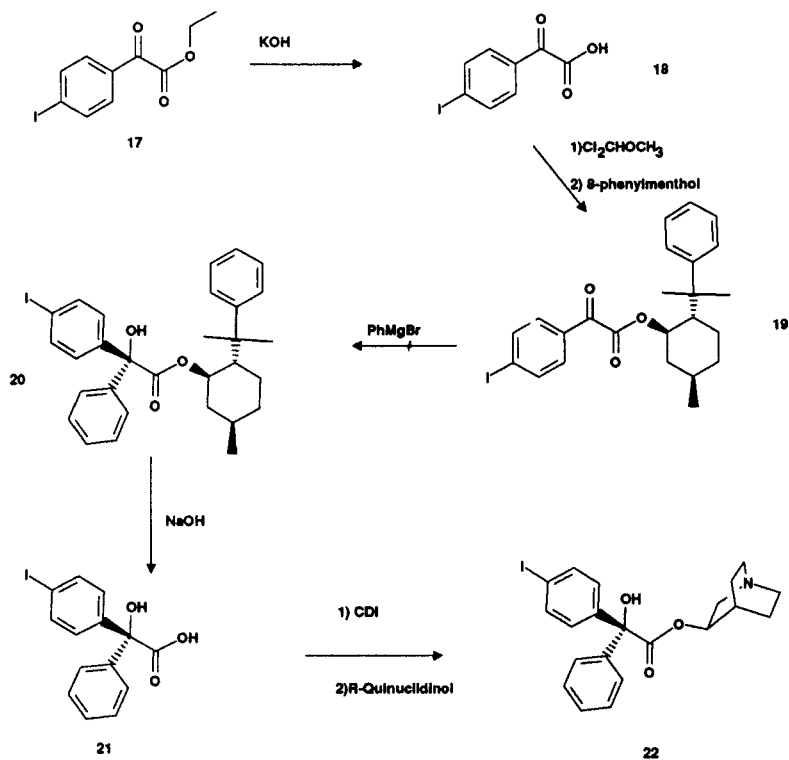
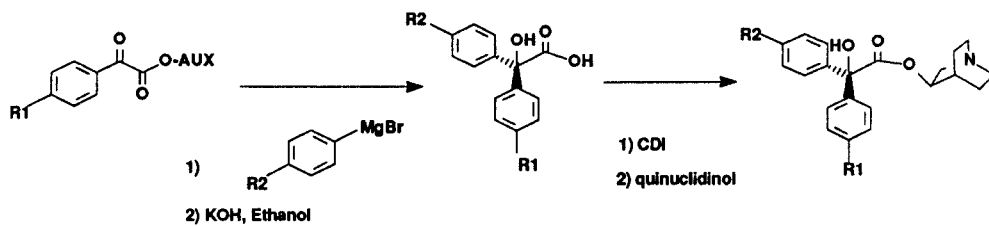
- <sup>1</sup>Rzeszotarski W.J.; Eckelman W.C.; Francis B.E.; Simms D.A.; Gibson R.E.; Jagoda E.M.; Grissom M.P.; Eng R.R.; Conklin J.J.; Reba R.C.--*J. Med. Chem.* **27**: 156-160 (1984). Gibson R.E.; Weckstein D.J.; Jagoda E.M.; Rzeszotarski W.J.; Reba R.C.; Eckelman, W.C.--*J. Nucl. Med.* **25**: 214-222 (1984). Eckelman W.C.; Reba R.C.; Rzeszotarski W.J.; Gibson R.E.; Hill T., Holman B.L.; Budinger T.; Conklin J.J.; Eng R.; Grissom M.P.--*Science* **223**, 291-293 (1984). Holman L.B.; Gibson R.E.; Hill T.C.; Eckelman W.C.; Albert M.; Reba R.C.--*J. Am. Med. Assoc.* **254**: 3063-3066(1986).
- <sup>2</sup>Meyerhoffer A.--*J. Med. Chem.* **15**(9): 994-995(1972).
- <sup>3</sup>Cohen V.I.; Rzeszotarski W.J.; Gibson R.E.; Fan L.H.; and Reba R.C.--*J. Pharmaceutical Sciences* , **78**(10): 833-836(1989).
- <sup>4</sup>Gibson R.E.; Schneidau T.A.; Cohen V.I.; Sook V.; Ruch J.; Melograna J.; Eckelman W.C.; Reba R.C.--*J. Nucl. Med.* **30**: 1079-1087(1989).
- <sup>5</sup>Zeeberg B.R., Gitler M.S., Baumgold J., de la Cruz R.A., Reba R.C.--*Biochem. Biophys. Res. Comm.* , **179**(2): 768-775(1991).
- <sup>6</sup>Inch T.D.; Green D.M.; Thompson P.B.J.--*J. Pharm. Pharmac.* , **25**: 359-370(1973).
- <sup>7</sup>Whitesell J.K.--*Acc.Chem.Res.* **18**: 280-284(1985).
- <sup>8</sup>Kiesewetter D.O.--Abstract--33rd National Organic Chemistry Symposium, Bozeman MT, (1993).

05/24/93

Kiesewetter

2

Scheme 1.

Scheme 2. Aux = 8-phenylmenthyl. R1 or R2 = H, CH<sub>2</sub>F, CH<sub>2</sub>CH<sub>2</sub>F, CH<sub>2</sub>CH<sub>2</sub>CH<sub>2</sub>F



05/24/93

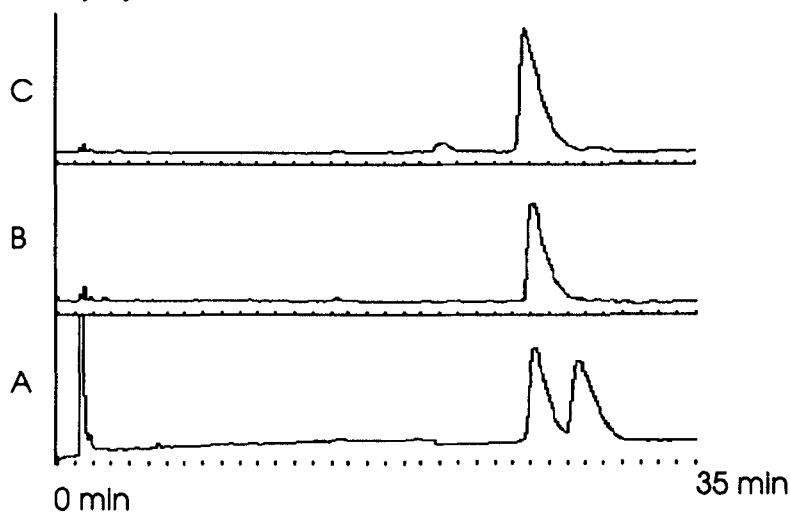
Kiesewetter

3

Table 1. In vitro affinities ( $K_i$ ) determined in a 5 point binding curve (NOVASCREEN) in the three major muscarinic tissue subtypes. The first configuration refers to the quinuclidinyl center. Numbers in parenthesis are standard errors.

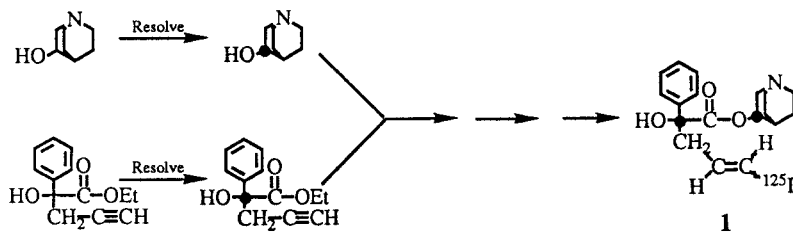
Compound	M1 (nM)	M2 (nM)	M3 (nM)
R,RS FluoroPropyl QNB	0.52 (50%)	4.93 (44%)	38 (15%)
R,S-FluoroPropyl QNB	0.20 (99%)	0.38 (42%)	59.4 (9%)
R,R-FluoroEthyl QNB	0.84 (8%)	7.6 (17%)	>10,000
R,S-FluoroEthyl QNB	0.26 (52%)	0.31 (24%)	84.7(4%)
R,RS-FluoroMethyl QNB	0.44 (39%)	3.55 (38%)	6.6 (14%)
S,RS-FluoroMethyl QNB	647 (49%)	14.2 (72%)	163 (11%)
S,S-FluoroMethyl QNB	2.9 (4%)	16.7 (9%)	9.5 (15%)
R,R-IodoQNB	0.34 (24%)	4.2 (21%)	8.1 (29%)
S,S-IodoQNB	4.6 (8%)	9.0 (4%)	40.5 (8%)

Figure 1. HPLC of IQNB showing diastomeric separation. Column Axxiom C-18 (4.6 x 250 mm). Eluant: 70%  $\text{CH}_3\text{CN}$ , 30% (5 mM  $\text{NaH}_2\text{PO}_4$ , 5 mM  $\text{Et}_3\text{N}$ ) 1.5 mL/min. A: racemic IQNB; B: [R,R] IQNB from present work; C: [R,R] IQNB authentic from Nordion.



**Preparation and Biological Evaluation of the Stereoisomers of 3-Quinuclidinyl  $\alpha$ -Hydroxy- $\alpha$ -([<sup>125</sup>I]-1-iodo-1-propen-3-yl)- $\alpha$ -phenylacetate (IQNP). A Novel Ligand for the Imaging of Muscarinic Receptors by SPECT.** McPHERSON D. W.<sup>\*</sup>; Lambert, C. R.; Jahn, K.; Knapp, Jr., F. F. (Russ). Nuclear Medicine Group, Oak Ridge National Laboratory (ORNL), Oak Ridge, TN 37831-6229.

Muscarinic cholinergic receptors (m-AChR) play an essential role in many physiological and behavioral responses. Changes in m-AChR have been implicated in various disease states in addition to memory functions, learning and aging. These observations have stimulated interest in the possibility of imaging the distribution of cerebral m-AChR binding sites non-invasively *in vivo* with external imaging techniques. We have recently reported the preparation of a high affinity muscarinic antagonist, IQNP (**1**), which demonstrates *in vivo* selectivity and specificity for m-AChR (1). IQNP is an analogue of 3-quinuclidinyl benzilate (QNB), and is radioiodinated in high yield (> 60 %) with high specific activity from a tributylstannyl derivative. Since carbon-3 of the quinuclidinyl moiety and the carbon-2 of the acetate moiety are asymmetric centers, and there can be either an E and Z configuration around the double bond, there is the possibility of 8 stereoisomers. We have initiated the synthesis and biological evaluation of the various stereoisomers to determine the optimum stereochemistry which imparts the maximum affinity for m-AChR.



Scheme 1. Preparation of the various isomers of IQNP (1).

Since the R configuration of the quinuclidinyl moiety has been reported to be 100 time more active than the S configuration (2), initially 3-quinuclidinol was resolved and (E,Z)-(R)-3-quinuclidinyl (R,S)  $\alpha$ -hydroxy- $\alpha$ -([<sup>125</sup>I]-1-iodo-1-propen-3-yl)- $\alpha$ -phenylacetate [(E,Z)-(R) (R,S)-IQNP] was prepared as shown in Scheme 1 for evaluation in female rats. The results of our study are shown in Table 1 and illustrate that uptake in receptor rich areas of the brain (cortex, striatum) is twice the uptake observed with the racemic mixture in these regions, after 6 hours.

Also, through careful separation of the racemic mixture utilizing a silica gel flash column with 98:2:1 chloroform:methanol:ammonium hydroxide mobile phase, we were able to isolate the E-(R,S) (S)-, (E)-(R,S) (R)-, and (Z)-(R,S) (R)- isomers of IQNP. The iodine-125-labeled isomers were evaluated in female rats and results of these studies (Table 1) demonstrate that the (E)-(R,S) (S) isomer washes out quickly from receptor rich areas while the (E)- and (Z)-(R,S) (R) isomers are retained in the cortex and striatum. The major difference observed in the (E) and (Z) isomers of (R,S) (R)-IQNP is the relative uptake of activity in the heart and cerebellum. The heart to blood ratios of the (E) and (Z)-isomers are 1.0 to 1 and 2.5 to 1, respectively, after 6 hours. The M<sub>2</sub> subtype is found in the heart and cerebellum (3), and these results suggest that the receptor subtype specificity may be influenced by the configuration around the double bond.

\*The submitted manuscript has been authored by a contractor of the U.S. Government under contract No. DE-AC05-84OR21400. Accordingly, the U.S. Government retains a nonexclusive, royalty-free license to publish or reproduce the published form of this contribution, or allow others to do so, for U.S. Government purposes.\*

The R and S isomers of  $\alpha$ -hydroxy- $\alpha$ -phenyl- $\alpha$ -(1-propyn-3-yl)acetic acid were resolved using quinidine and quinine. The E-(R)(R)- and E-(R)(S)-isomers of IQNP were then prepared using analogous methods that had been used in the preparation of the racemic mixture (Scheme 1), and characterized by NMR, HPLC, elemental analysis and specific rotation. (E)-(R) (R)- and (E)-(R) (S)-[<sup>125</sup>I]-QNP were prepared and evaluated in female rats and the results are shown in Figures 2 and 3, respectively. As expected, (E)-(R) (R)-[<sup>125</sup>I]-QNP demonstrates high uptake in receptor rich areas of the brain while uptake in the heart, although high initially, washes out over the time period of the experiment. (E)-(R) (S)-[<sup>125</sup>I]-QNP demonstrates rapid washout from these same areas. The dramatic effect of the absolute configuration of the asymmetric acetate center was unexpected. Work is continuing on the preparation and evaluation of the (Z)-(R) (R)- and (Z)-(R) (S) isomers of IQNP.

These results demonstrate that (E)-(R) (R)-[<sup>125</sup>I]-QNP has high uptake and low nonspecific binding in cerebral m-AChR rich areas and is an excellent candidate for further development as an agent for *in vivo* detection of m-AChR by SPECT.

Research at ORNL supported by the Office of Health and Environmental Research, U.S. Department of Energy, under contract DE-AC05-84OR21400 with Martin Marietta Energy Systems, Inc.

Table 1. Evaluation of Various Isomers of [<sup>125</sup>I]-QNP (1) in Female Fischer Rats at 6 Hours (n=5).

Organ	Racemic IQNP	(E,Z)-(R) (R,S)IQNP	(E)-(R,S) (S)IQNP	(E)-(R,S) (R)IQNP	(Z)-(R,S) (R)IQNP	(E)-(R)(R) IQNP	(E)-(R)(S) IQNP
Cortex	0.47 ±0.06	0.84 ±0.17	0.06 ±0.00	0.71 ±0.05	0.73 ±0.18	1.38 ±0.31	0.04 ±0.00
Striatum	0.41 ±0.07	0.72 ±0.09	0.03 ±0.02	0.56 ±0.05	0.59 ±0.14	1.22 ±0.20	0.02 ±0.02
Cerebellum	0.06 ±0.01	0.08 ±0.02	0.02 ±0.01	0.03 ±0.01	0.17 ±0.04	0.04 ±0.01	0.01 ±0.01
Heart	0.17 ±0.02	0.24 ±0.05	0.12 ±0.02	0.13 ±0.01	0.56 ±0.12	0.10 ±0.02	0.06 ±0.01
Blood	0.21 ±0.02	0.14 ±0.03	0.27 ±0.02	0.16 ±0.02	0.20 ±0.04	0.09 ±0.02	0.11 ±0.01

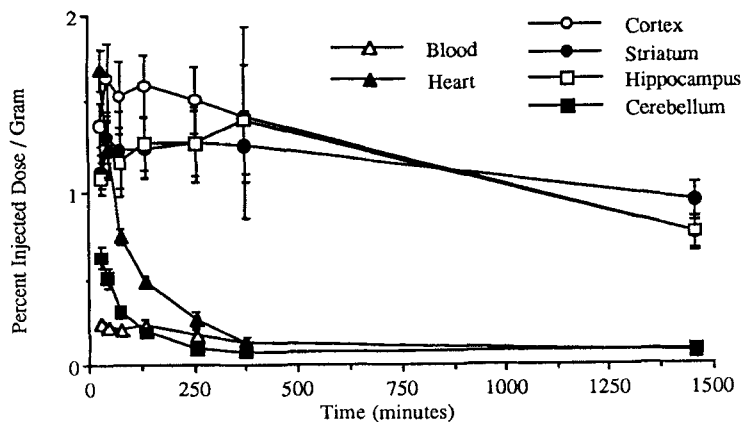


Figure 1. Biodistribution of (E)-(R) (R)[125I]QNP in Fischer Female Rats (n=5).

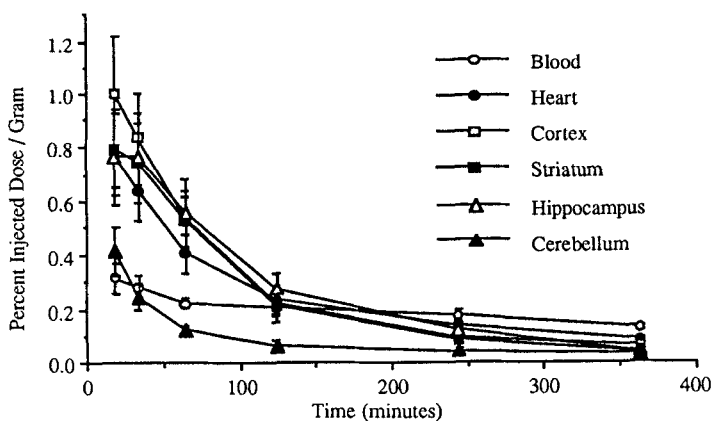


Figure 2. Biodistribution of (E)-(R) (S)[125I]QNP in Fischer Female Rats (n=5).

References

1. McPherson, D.W., DeHaven-Hudkins, D.L., Callahan, A.P., and Knapp, F.F., Jr., *J. Med. Chem.*, **36**, 848-854 (1993).
2. Meyerhoffer, A., *J. Med. Chem.*, **15**, 994-995 (1972).
3. Swada, Y., Hiraga, S., Francis, B., Patlak, C., Pettigrew, K., Ito, K., Owens, E., Gibson, R., Reba, R., Eckelman, W., Larson, S., and Blasberg, R.G., *J. Cereb. Blood Flow Metab.*, **10**, 781-807 (1990).

**SYNTHESIS OF [CARBONYL  $^{11}\text{C}$ ] AF-DX 384, A SELECTIVE ANTAGONIST OF  $M_2$  RECEPTORS FOR POSITRON EMISSION TOMOGRAPHY STUDIES.**

LASNE M.C.; BARRÉ L.+; HUARD C.; DUCANDAS C.; and MacKENZIE E. T.++

Unité de Recherche Associée au CNRS, Institut des Sciences de la Matière et du Rayonnement, 6 Bd du Maréchal Juin, 14050 Caen - Université de Caen-Basse Normandie ; + CEA, DSV/DPTE, ++CNRS F019, Centre Cyceron, Bd Henri Becquerel, 14021 Caen, FRANCE

Muscarinic receptors mediate the actions of the neurotransmitter acetylcholine in the central and peripheral nervous systems. The localization and quantification of these receptors in the living brain using PET may provide valuable information about receptor changes in various patho-physiological conditions and especially in neurodegenerative disorders such as Alzheimer's disease. In this pathological situation, the cerebral presynaptic  $M_2$  muscarinic receptor population is considerably reduced<sup>1</sup>. Several ligands labelled with a positron emitter have been synthesized to visualize the cholinergic system *in vivo*<sup>2</sup>. To our knowledge none of them are selective towards the  $M_2$  receptors. Recently, AF-DX 384 [5,11-dihydro-11(((2-(dipropylamino)methyl-1-piperidinyl)ethyl)aminocarbonyl)-6H-pyrido(2,3-b)(1,4)-benzodiazepinone)] was prepared<sup>3</sup>. Its binding to muscarinic receptors was studied in the rat heart<sup>4</sup> and brain<sup>5</sup> using the tritiated form. Its binding affinity in the low nanomolar range and its high selectivity towards  $M_2$  receptors make AF-DX 384 a good candidate for PET studies. We report here our first results concerning its labelling with carbon-11.

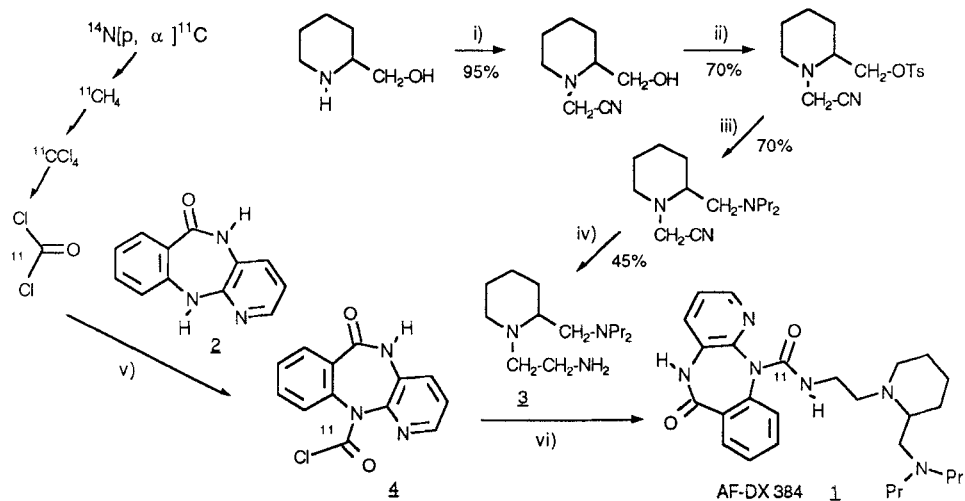
AF-DX 384 **1** (scheme 1) is a polyfunctional compound bearing an unsymmetrical urea function. Ureas usually result from the reaction of amines with phosgene. The reactions are rapid and they have successfully been applied to the preparation of [carbonyl- $^{11}\text{C}$ ] ureas using [ $^{11}\text{C}$ ] phosgene<sup>6</sup> as the labelled precursor. Tracers with a high specific radioactivity could be obtained when [ $^{11}\text{C}$ ] phosgene was prepared by oxidation of carbon tetrachloride obtained by chlorination of methane<sup>7</sup>.

The different steps of the synthesis of AF-DX 384 **1** are shown in scheme 1. The benzodiazepinone **2** was prepared according to a known procedure<sup>3</sup>. An original synthesis of the piperidine **3** was developed starting from racemic piperidinemethanol. The reaction of unlabelled phosgene with benzodiazepinone **2** and the condensation of the chlorocarbamate **4** with the piperidine **3** were studied under different conditions (time, solvent, temperature). The results showed that the chlorocarbamate **4** was instantaneously formed when the reaction was carried out in dioxane. It is stable at room temperature and leads to the starting benzodiazepinone **2** on silica gel column. It is however unreactive towards an excess of benzodiazepinone and no formation of symmetrical urea was observed. An efficient and rapid condensation of **4** with the piperidine **3** was achieved in acetonitrile.

[ $^{11}\text{C}$ ] phosgene prepared according to the previously described methods<sup>7</sup> was introduced sequentially over 20 min at room temperature into a solution of benzodiazepinone **2** (4 mg, 18.9  $\mu\text{mol}$ ) in dioxane. The mixture was then transferred under nitrogen in a vial containing the piperidine **3** (5 mg, 20.7  $\mu\text{mol}$ ) in acetonitrile. After heating the mixture at 45°C for 5 min, [ $^{11}\text{C}$ ] AF-DX 384 **1** was formed in 25-40% yield from [ $^{11}\text{C}$ ] phosgene. Under the same conditions but with the stable isotope, AF-DX 384 was obtained in 30% yield after purification by chromatography.

The compound **1** was identified by comparison of its  $R_f$  in radioTLC with three different eluting systems [ $R_f$ : 0.62 ( $\text{CH}_2\text{Cl}_2$ : MeOH, 80:20, v/v), 0.35 (acetone: MeOH, 70:30, v/v)

0.48 (AcOEt: MeOH, 40: 60, v/v)] and by HPLC [normal phase,  $\lambda$ : 254 nm, 4 ml.min<sup>-1</sup>, retention time : 1 : 6.9 ; 2 : 5.5 min]. The radioTLC analysis of the crude product showed the formation of three labelled side products (Rf 0.9, 0.45 and 0.2 in CH<sub>2</sub>Cl<sub>2</sub>: MeOH, 80: 20, v/v) in a ratio of about 3:1:3 the structure of which being not yet assigned. Work is in progress to identify these compounds and to optimize the reaction conditions in order to obtain a ligand with a high specific radioactivity.

Scheme 1 : synthesis of [carbonyl <sup>11</sup>C] AF-DX 384

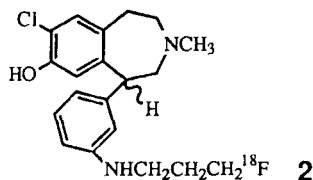
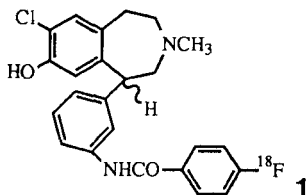
i) ClCH<sub>2</sub>CN, Et<sub>3</sub>N, EtOH, 78°C, 15h ii) TsCl, Py, RT, 24h iii) Pr<sub>2</sub>NH, 105°C, 2h iv) LiAlH<sub>4</sub>, THF, 0°C, 2h v) dioxane, RT, 3 min vi) acetonitrile, 45°C, 5 min.

## References

- Doods H. N. *et al.* - Life Sciences **52**: 497 (1993)
- a) [<sup>11</sup>C] dexetimide: Dannals R. F. *et al.* - Appl. Radiat. Isot. **39**: 291 (1988) ; b) [<sup>11</sup>C] QNB: Prenant C. *et al.* - J. Labelled Comp. Radiopharm. **27**: 1257 (1989) ; c) N- [<sup>11</sup>C] methyl-scopolamine: Mulholland G. K. *et al.* - Appl. Radiat. Isot. **39**: 372 (1988) ; Vora M. M. *et al.* - J. Labelled Comp. Radiopharm. **20**: 1229 (1983) ; d) [<sup>18</sup>F] fluorodexetimides: Wilson A. A. *et al.* - Labelled Comp. Radiopharm. **28**: 117 (1990) ; Hwang D.R. *et al.* - Nucl. Med. Biol. **18**: 247 (1991) ; e) [N-<sup>11</sup>C-methyl]-benztropine : Dewey S. L. *et al.* - J. Neuroscience Res. **27**: 569 (1990) ; f) [<sup>11</sup>C] oxyphenonium iodide: Vlek J. W. *et al.* - Appl. Radiat. Isot. **41**: 453 (1990) ; g) [<sup>18</sup>F] vesamicol derivatives: Rogers G. *et al.* - J. Labelled Comp. Radiopharm. **32**: 486 (1993); Mulholland G. K. *et al.* - J. Labelled Comp. Radiopharm. **32**: 487 (1993)
- Engel W., Eberlein W., Mihm G., Trummelitz G., Mayer N., and De Jonge A. - Ger. Offen. DE 3, 643, 666 (1988); Chem. Abstr. **110**: 39029f (1989)
- Antzeroth M., and Mayer N. - Biochem. Pharmacol. **40**: 1674 (1990)
- Aubert I, Cécyre D, Gauthier S, and Quirion R - Eur. J. Pharmacol. **217**: 173 (1992)
- see i.e: Conway T., and Diksic M. - Appl. Radiat. Isot. **42**: 441 (1991)
- a) Landais P., and Crouzel C. - Appl. Radiat. Isot. **38**: 297 (1987) ; b) Brady F. *et al.* - Appl. Radiat. Isot. **42**: 621 (1991)

**In Vivo Evaluation of Fluorinated Benzazepines as Selective, High Affinity PET Tracers for Dopamine D-1 Receptors.** Yang, Z-Y and Mukherjee, J. Department of Radiology, University of Chicago, Chicago, IL 60637

**Introduction:** Development of [<sup>18</sup>F]fluorinated derivatives of benzazepines as radioligands for imaging of the D-1 receptor by PET has attracted attention due to the advantages of fluorine-18 (Mach et al., 1992; Moerlein et al., 1989; Teng et al., 1991). We have previously reported fluoroalkyl and fluoroaryl derivatives of SCH 38548 as high affinity and selective ligands for the D-1 receptor (Mukherjee et al., 1992). Here we report *in vivo* studies of two of the radiotracers, *N*-(4-[<sup>18</sup>F]fluorobenzoyl)SCH 38548, **1** and *N*-(3-[<sup>18</sup>F]fluoropropyl)SCH 38548, **2**.



**Pharmacology:** Receptor binding affinities of *N*-(4-[<sup>18</sup>F]fluorobenzoyl)SCH 38548 and *N*-(3-fluoropropyl)SCH 38548 were obtained *in vitro* on rat striatal membranes by competition experiments for D<sub>1</sub> (labeled with <sup>3</sup>H-SCH 23390) IC<sub>50</sub>±SD = 0.55±0.33 and 4.80±3.60 nM, respectively. Affinities for the dopamine D<sub>2</sub> and serotonin 5HT<sub>2</sub> receptor sites were very weak (Mukherjee et al., 1992). The selectivity of *N*-(3-fluoropropyl)SCH 38548 for D<sub>1</sub> receptor-sites is better than SCH 23390 and SCH 39166 (Chipkin et al., 1988).

**Radiosynthesis:** For purposes of [<sup>18</sup>F]fluoroalkylation, [<sup>18</sup>F]fluoropropyl iodide was produced by reacting *neq* [<sup>18</sup>F]fluoride/kryptofix/ K<sub>2</sub>CO<sub>3</sub> with diiodopropane in CH<sub>3</sub>CN at 75°C followed by the addition of SCH 38548. [<sup>18</sup>F]fluoropropylation was carried out in dimethylformamide at 110°C. Purifications (RP-HPLC) of *N*-[<sup>18</sup>F]fluoropropyl SCH 38548 **2** provided apparent specific activities of 700-900 Ci/mmol. For *N*-p-[<sup>18</sup>F]fluorobenzoylation of SCH 38548, p-[<sup>18</sup>F]fluorobenzoyl fluoride was produced from p-nitrobenzaldehyde in three steps (nucleophilic [<sup>18</sup>F]fluoride rxn, oxidation by Jones reagent followed by treatment with DAST). *N*-p-[<sup>18</sup>F]fluorobenzoyl derivative **1** was obtained in 6-10% yields in specific activities of 0.8-1.0 Ci/μmol.

**In vivo studies:** Brain distribution studies of *N*-(3-[<sup>18</sup>F]fluorobenzoyl)SCH 38548 and *N*-(3-[<sup>18</sup>F]fluoropropyl)SCH 38548 were carried out in male Sprague-Dawley rats after iv administration of the radiotracer. *N*-(3-[<sup>18</sup>F]fluoropropyl)SCH 38548 showed good striatal uptake and retention (0.64 % injected dose/g at 30 min, 0.57 % at 60 min and 0.52 % at 120 min post injection) whereas cerebellum (a dopamine D<sub>1</sub> receptor deplete region) showed little retention of the radiotracer. Specific to nonspecific (striata/cerebellum) ratio of 6.10, 7.61 and 12.0 at 30, 60 and 120 min postinjection respectively, were obtained. This striata/cerebellum ratio for the tracer was abolished when the D<sub>1</sub> receptor sites were blocked by preadministration of SCH 23390 (2 mg/kg, 15 minutes prior to the administration of the radiotracer). *N*-(3-[<sup>18</sup>F]fluorobenzoyl)SCH 38548 showed specific uptake in the striata with ratios (striata/cerebellum) approaching 8, 2 hours post-injection. However, biodistribution data with this derivative were not completely reproducible when repeated on several other occasions (striata/cerebellum ratios fluctuated in the range of 4 to 8, two hours p.i.). Preliminary PET studies in rhesus monkeys with *N*-(3-[<sup>18</sup>F]fluorobenzoyl)SCH 38548 showed no striatal uptake and the compound cleared from the brain rather rapidly. Defluorobenzoylation seems to be a major metabolic pathway that may be responsible for the poor *in*

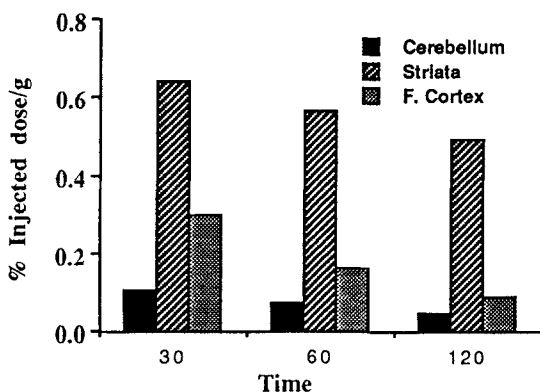
*in vivo* behavior of this derivative. On the other hand, *N*-(3-[<sup>18</sup>F]fluoropropyl)SCH 38548 seems very promising in preliminary PET studies in rhesus monkeys. The tracer was taken up in the striata and showed retention in this region over the cerebellum. No defluorination was observed in the PET scan. Further experiments are now being carried out to characterize *in vivo* behavior of *N*-(3-[<sup>18</sup>F]fluoropropyl)SCH 38548.

**Table-1:** Biodistribution of *N*-(3-[<sup>18</sup>F]fluoropropyl)SCH 38548 in Rats\*

Organ	30 min	60 min	120 min
Heart	0.22±0.13	0.16±0.06	0.05±0.01
Muscle	10.3±3.38	12.3±8.60	2.80±0.21
Spleen	0.25±0.03	0.15±0.02	0.08±0.00
Bladder	0.29±0.31	0.12±0.03	0.09±0.05
Kidney	1.71±0.29	1.10±0.24	0.78±0.09
Lung	1.52±0.17	1.12±0.48	0.38±0.05
Liver	9.04±0.84	6.59±0.31	5.78±0.31
Blood	1.71±0.65	0.98±0.07	0.57±0.05
Bone	8.84±4.40	12.9±1.16	17.9±1.68
Brain	0.33±0.07	0.27±0.03	0.17±0.01

\* Post-iv injection, % injected dose/organ, average of 3 rats ± sample std. dev.

**Figure-1:** Rat brain distribution of *N*-(3-[<sup>18</sup>F]fluoropropyl)SCH 38548. Data are averages of three rats for each time-point.



#### References:

- Chipkin, R.E., L.C. Iorio, V.L. Coffin, R.D. McQuade, J.G. Berger and A. Barnett. *J. Pharm. Expt. Therap.* **247**, 1093 (1988).
- Mach, R.H., P.A. Nowak, P.H. Evora and R.L. Ehrenkauffer. *J. Nucl. Med.* **33**, 829 (1992).
- Moerlein, S.M., Lannoye, G.S. and Welch, M.J. *J. Nucl. Med.* **30**:931 (1989).
- Mukherjee, J., Z.-Y. Yang, B.D. Perry and M. Cooper. *J. Nucl. Med.* **33**, 829 (1992).
- Teng, R-R., L-Q. Bai, C-Y. Shiue, S.L. Dewey, C.D. Arnett, A.P. Wolf and R.J. Hitzemann. *Nucl. Med. Biol.* **17**, 811 (1990).



**Acknowledgements:** We like to thank financial support from Department of Energy (contract No. DE-FG02-86ER60438) and the Scottish Rite Schizophrenia Foundation. Technical assistance of Dr. M.K. Das, X.-H. Ouyang, P. Nicole, Dr. S. Kronmal and T. Brown is gratefully acknowledged.

PREPARATION OF [<sup>11</sup>C] NNC 22-0010 AND [<sup>76</sup>Br] NNC 22-0010.  
SELECTIVE D<sub>1</sub> DOPAMINE RECEPTOR ANTAGONISTS FOR PET.

Foged<sup>1,2</sup>, C.; Halldin<sup>1</sup>, C.; Loc'h<sup>3</sup>, C.; Mazière<sup>3</sup>, B.; Karlsson<sup>1</sup>, P.; Mazière<sup>3</sup>, M.; Swahn<sup>1</sup> C-G. and Farde<sup>1</sup>, L. <sup>1</sup>Department of Psychiatry and Psychology, Karolinska Institute, Stockholm, Sweden, <sup>2</sup>Novo Nordisk A/S, Pharmaceuticals Division, Denmark and <sup>3</sup>Service Hospitalier Frédéric Joliot, CEA, Orsay, France.

[<sup>11</sup>C]SCH 23390, [<sup>11</sup>C]SCH 39166 and [<sup>11</sup>C]NNC 756 have been prepared and used as radio ligands to visualize dopamine D<sub>1</sub> receptors in the living human brain using PET (1-4). NNC 22-0010 ((+) 8-chloro-5-(5-bromo-2,3-dihydrobenzofuran-7-yl)-7-hydroxy-3-methyl-2,3,4,5-tetrahydro-1H-3-benzazepine) is a new dopamine D<sub>1</sub> receptor antagonist, with a high affinity *in vitro* (IC<sub>50</sub> 1.5 nM) and a 200-fold lower binding to serotonin receptors. NNC 22-0010 contains both a N-methyl group and a bromine, which allows isotopic labelling with either <sup>11</sup>C or <sup>76</sup>Br. Alternative labelling may be of value for radioligand development, for the examination of brain kinetics and metabolism.

[<sup>11</sup>C]NNC 22-0010 was labelled by N-alkylation of the free base of the secondary amine with [<sup>11</sup>C]methyl iodide in acetone at 90 °C for 4 minutes (Scheme 1). The purification was performed by semi-preparative straight-phase HPLC with a total radiochemical yield of 40% (from EOB and decay corrected), with a total synthesis time of 30-35 minutes and with radiochemical purity > 99%. [<sup>76</sup>Br]NNC 22-0010 was synthesized using the iodine precursor (Scheme 2). The exchange reaction was performed at 165 °C for one hour in a sealed vial in the presence of Cu<sup>+</sup> and an excess of reducing agents (gentisic acid, ascorbic acid and citric acid) according to Mertens procedure (5-6). For purification, the reaction mixture was poured on a C18 cartridge and all polar by-products washed out with water. The halogeno compounds were eluted with methanol. [<sup>76</sup>Br]NNC 22-0010 was separated from the iodo precursor by subsequent semi-preparative reversed-phase HPLC purification. The radiochemical yield was 60% after purification, and the radiochemical purity > 98%.

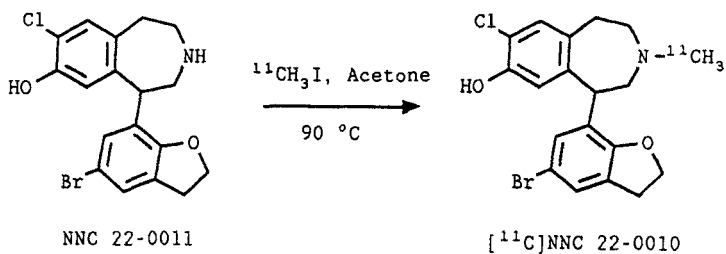
*In vivo* biodistribution studies in rats with [<sup>76</sup>Br]NNC 22-0010 demonstrated a high striatum to cerebellum ratio (S/C = 19), 3 hours after injection. Co-injection with SCH23390 reduced the striatal uptake to that of the cerebellum. Spiperone had no effect on the S/C ratio, showing the specificity of the binding. Also *ex vivo* autoradiography studies demonstrated high specific binding in the striatum.

In a PET study in Cynomolgus monkey with [<sup>11</sup>C]NNC 22-0010 there was a rapid uptake in the brain. The S/C ratio reached a value of about 2.5. Displacement with SCH 23390 reduced the striatal uptake almost to that of the cerebellum.

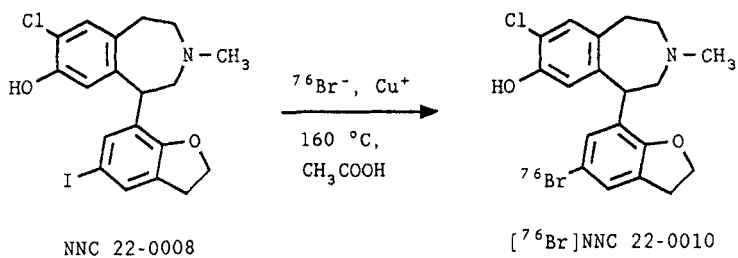
A PET experiment in baboon with [<sup>76</sup>Br]NNC 22-0010 showed a similar uptake in the brain as described above. The S/C ratio of 2.5 at 30 minutes remained constant for more than 1 hour. The half-life in striatum was 90 minutes.

1. Halldin C., Stone-Elander S., Farde L., Ehrin E., Fasth K.-J. Långström B. and Sedvall G. — *Appl. Radiat. Isot.* 37, 1039-1043 (1986).
2. Farde L., Halldin C., Stone-Elander S. and Sedvall G. — *Psychopharmacology* 92, 278-284 (1987).
3. Halldin C., Farde L., Barsedt A. and Sedvall G. — *Appl. Radiat. Isot.* 42, 451-455 (1991).
4. Halldin C., Hansen K., Foged C., Grønvald F.C. and Farde L. — *J. Nucl. Med.* 32, 934-935 (1991).
5. Mertens J., Vanryckeghem W., Gysemans M. *et al.* *Eur. J. Nucl. Med.* 13, 380 (1987).
6. Loc'h C., Guillaume M., Stulzaft D. *et al.* *J. Lab. Comp. Radiopharm.* 32, 291 (1993).

## Scheme 1



## Scheme 2



**Synthesis of [<sup>18</sup>F]-N-3-Fluoropropyl-2-Thienylspiroperidol: A New Radioligand for PET Study of the Dopamine D<sub>2</sub> Receptor**

GOODMAN, M.M.; KABALKA, G.W.; GOTTSICK, T.; WATERHOUSE, R.N.; and MEYER, M.A. Biomedical Imaging Center, University of Tennessee at Knoxville, Knoxville, TN 37920 USA

Abnormalities in CNS dopaminergic neurotransmission have been implicated in a variety of psychomotor disorders such as Parkinson's disease, Huntington's chorea and schizophrenia. A number of analogs of spiroperidol, a potent antipsychotic with a high (nanomolar) affinity for dopamine D<sub>2</sub> receptors, have been synthesized as radiotracers for imaging and quantifying dopamine D<sub>2</sub> receptor sites in the brain using PET imaging techniques. The most extensively evaluated positron emitting analogs of spiroperidol are [<sup>18</sup>F]spiroperidol (1), [<sup>18</sup>F]- or [<sup>11</sup>C]-N-methylspiroperidol (2,3), [<sup>18</sup>F]-N-(2-fluoroethyl) spiroperidol (4), and [<sup>18</sup>F]-N-(3-fluoropropyl)spiroperidol (5). In vivo imaging studies of dopamine D<sub>2</sub> receptor sites with this family of radiotracers in human and non human primates demonstrated very high specific uptake in the dopamine-rich striatal tissue and low nonspecific uptake in the dopamine-poor cerebellum. However, an undesired property accompanying very high striatal uptake of positron emitting analogs of spiroperidol is high affinity for serotonin 5-HT<sub>2</sub> receptors (also present in striatal tissue).

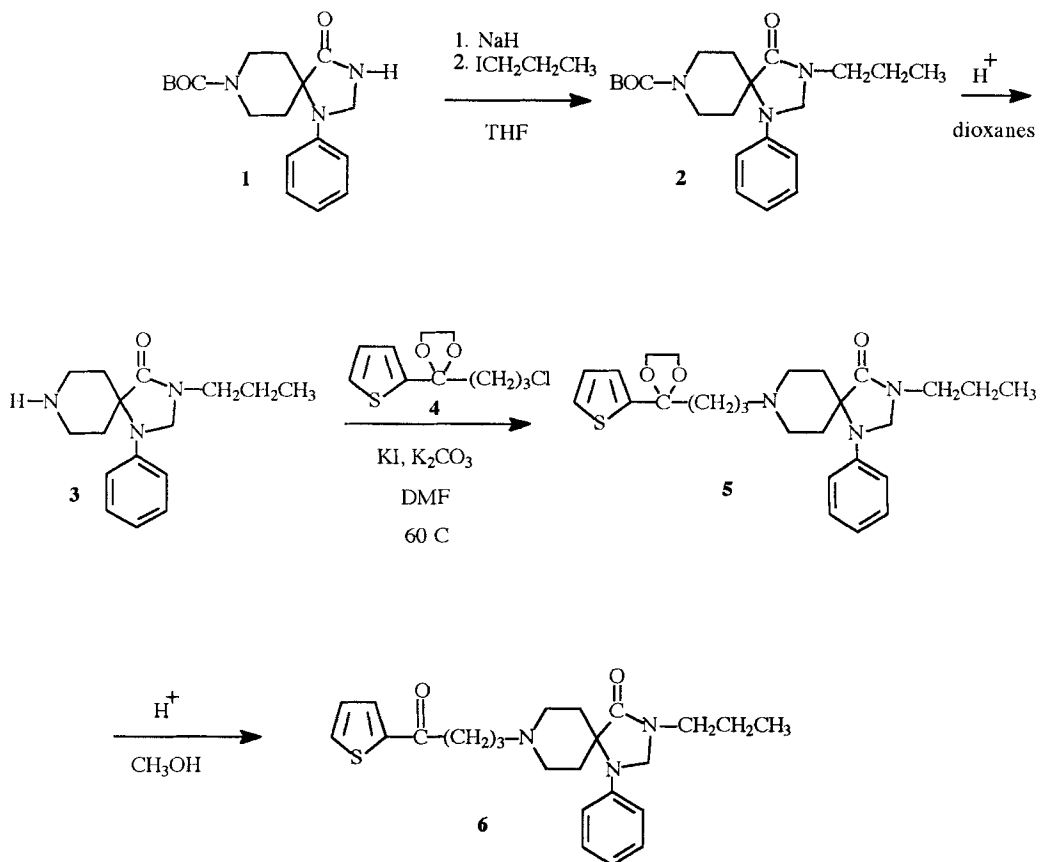
In order to provide a positron emitting analog of spiroperidol with high and selective affinity for the dopamine D<sub>2</sub> receptor, we synthesized and evaluated several N-substituted-2-thienylspiroperidols. A new analog, 3-N-propyl-2-thienylspiroperidol (Scheme 1), was found to be potent in inhibiting binding of [<sup>3</sup>H]sulpiride to rat striatal tissue (100%) but not potent in inhibiting [<sup>3</sup>H]ketanserin, a 5-HT<sub>2</sub> receptor ligand to rat cortical tissue (18%) at 10<sup>-8</sup>M. These findings prompted us to synthesize [<sup>18</sup>F]-N-3-fluoropropyl-2-thienylspiroperidol, an isostere of N-propyl-2-thienylspiroperidol, as a potential PET dopamine D<sub>2</sub> receptor imaging agent.

The [<sup>18</sup>F]-N-3-fluoropropyl-2-thienylspiroperidol was prepared in the synthetic approach described in Scheme 2. The [<sup>18</sup>F]-N-3-fluoropropyl-2-thienylspiroperidol was labeled by reacting N-3-bromopropyl-2-thienylspiroperidol with no-carrier-added K<sup>18</sup>F/K222 in acetonitrile at 90°C for 30 min. The [<sup>18</sup>F]-N-3-fluoropropyl-2-thienylspiroperidol was obtained in 17% radiochemical yield (EOS).

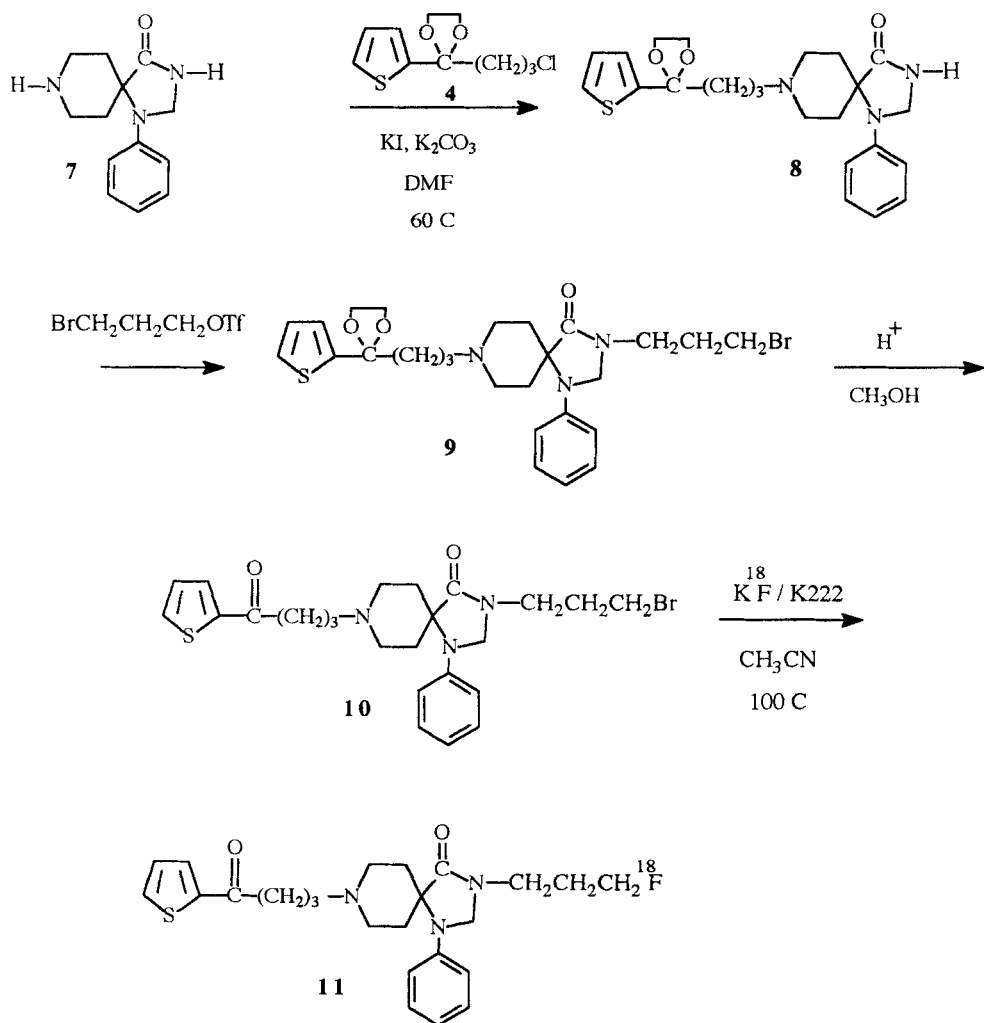
Research supported by the Office of Health and Environmental Research, U.S. Department of Energy and the National Institute of Mental Health.

References

1. Kilbourn, M.R., Welch, M.J., Dence, C.S., et al. - *Int.J.Appl.Isot.* **35**: 591-598 (1984)
2. Shieu, C.-Y., Fowler, J.S., Wolfe, A.P., et al. - *J.Nucl.Med.* **27**: 226-234 (1986)
3. Wagner, H.N. Jr., Bruns, H.D., Dannals, R.F., et al. - *Ann.Neurol.* **15** (suppl): S79-S84 (1984)
4. Coenen, H.H., Laufer, P., Stocklin, G., et al. - *Life Sci.* **40**: 81-88 (1987)
5. Welch, M.J., Katzenellbogen, J.A., Brodack, J.W., et al. - *Nucl.Med.Biol.* **15**: 83-97 (1988)



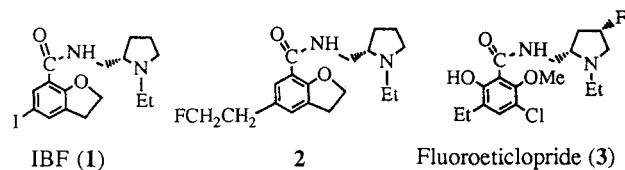
Scheme 1. Synthesis of N-propyl-2-thienylspiroperidol



Scheme 2. Synthesis of N-3-[F-18]fluoropropyl-2-thienylspiroperidol

**Synthesis of New Fluorine-18 Labeled Benzofuran Benzamide and Its *In Vivo* Evaluation as a Dopamine D2 Radioligand**SASAKI<sup>a</sup>, S.; TAKAO<sup>a</sup>, F.; MAEDA<sup>a</sup>, M.; FUKUMURA<sup>b</sup>, T.; MASUDA<sup>b</sup>, K.; and ICHIYA<sup>b</sup>, Y.<sup>a</sup>Faculty of Pharmaceutical Sciences and <sup>b</sup>Faculty of Medicine, Kyushu University, 3-1-1 Maidashi, Higashi-ku, Fukuoka 812, Japan

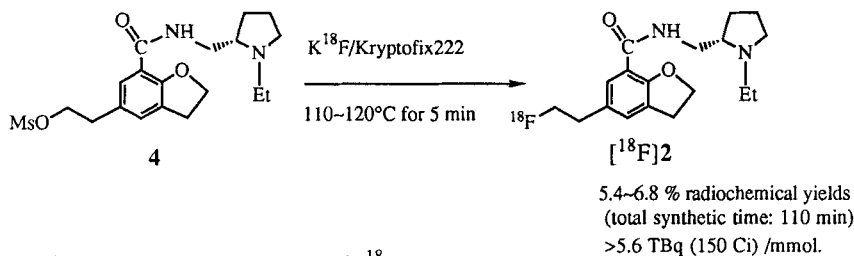
In the search for selective radioligands for *in vivo* imaging of neurotransmitter systems in the central nervous system (CNS), we synthesized [<sup>18</sup>F]fluorinated benzamide derivatives with *in vitro* affinity to D2 receptors (Table 1).<sup>1,2</sup> <sup>18</sup>F-Labeled eticlopride derivative ([<sup>18</sup>F]3) showed only moderate *in vivo* selectivity as illustrated by striatal/cerebellar radioactivity ratio of 5.2 in rats at 90 min, in spite of its high *in vitro* affinity.<sup>1</sup> In this paper, we wish to report that [<sup>18</sup>F]2, <sup>18</sup>F-fluoroethyl derivative of IBF (1), exhibited higher striatal/cerebellar radioactivity ratio of 12 in rats at 60 min, although it has lower *in vitro* affinity to D2 receptors (Table 1).

**Table 1.**

Compound	IC <sub>50</sub> (nM) <sup>a</sup>
IBF (1)	0.16
2	36
3	1.9

a) Concentration to inhibit specific binding of [<sup>3</sup>H]spiperone by 50%

The radiochemical synthesis was shown in Fig.1. No-carrier-added aqueous [<sup>18</sup>F]fluoride was prepared in an [<sup>18</sup>O]H<sub>2</sub>O enriched target (8 or 16%) using <sup>18</sup>O(p,n)<sup>18</sup>F nuclear reaction, and used to prepare K<sup>18</sup>F/Kryptofix222. [<sup>18</sup>F]Fluorination with the mesylate precursor 4 was performed in the absence of solvent in the analogous manner to the synthesis of [<sup>18</sup>F]3.<sup>1</sup> A single purification by HPLC with a normal phase column provided [<sup>18</sup>F]2 in 5.4~6.8 % radiochemical yields (total synthetic time: 110 min, uncorrected for decay) with high chemical and radiochemical purity, which specific activities were estimated to be larger than 5.6 TBq (150 Ci) /mmol.

**Fig 1.** Radiochemical Synthesis of [<sup>18</sup>F]5

A solution of [<sup>18</sup>F]2 in saline-5% ethanol was injected into rat tail veins, and the biodistribution at different times after the injection is summarized in Table 2. Initial uptake was cleared in almost all tissues except in the bone and striatum. The bone activity increased gradually to 1.05 %dose/g at 60 min, indicating slow defluorination *in vivo*. Although the radioactivity uptake in the striatum was not very high (0.40 % dose/g at 30 min), the radioactivity was clearly retained, and the striatal/cerebellar radioactivity ratio which corresponds to *in vivo* selectivity between receptor-rich and receptor-poor brain region reached to 12 at 60 min. In contrast to the fact that [<sup>18</sup>F]3 with higher *in vitro* affinity toward D2 receptors (Table 1) exhibited lower *in vivo* selectivity to striatum,<sup>1c</sup> it is interesting that [<sup>18</sup>F]2 with lower *in vitro* affinity achieved the higher striatal/cerebellar ratio. Cerebellum uptake which is used to estimate nonspecific binding is rapidly cleared with the use of [<sup>18</sup>F]2 from 0.20

%dose/g (5 min) to 0.02 %dose/g (60 min), whereas the clearance of [ $^{18}\text{F}$ ]3 was slower as shown by the change from 0.20 %dose/g (30 min) to 0.09 %dose/g (120 min).<sup>1c)</sup> Hence, less nonspecific binding of [ $^{18}\text{F}$ ]2 to cerebellum is attributable to its relatively high *in vivo* selectivity.

**Table 2.** Tissue Distribution of Radioactivity in Rats of [ $^{18}\text{F}$ ]Fluoroethylbenzofuran(2).<sup>a)</sup>

Tissue	Biodistribution			Inhibition <sup>b)</sup>	
	%dose/g			%dose/g after 30 min	
	5 min	30 min	60 min	control	Haloperidol
Brain	0.26±0.02	0.12±0.01	0.05±0.02	0.09±0.01	0.06±0.01
Striatum	0.33±0.01	0.40±0.05	0.24±0.12	0.30±0.01	0.06±0.01
Cerebellum	0.20±0.03	0.07±0.01	0.02±0.01	0.06±0.02	0.05±0.01
Cerebral cortex	0.29±0.02	0.12±0.04	0.02±0.02	0.08±0.01	0.07±0.01
Hippocampus	0.20±0.02	0.10±0.03	0.03±0.02	0.07±0.00	0.06±0.01
Blood	0.22±0.02	0.21±0.01	0.08±0.04	0.15±0.03	0.21±0.02
Bone	0.14±0.05	0.74±0.03	1.05±0.20	0.52±0.09	0.87±0.04
Lung	1.84±0.30	0.36±0.19	0.18±0.07	0.47±0.06	0.58±0.14
Liver	1.15±0.21	0.71±0.11	0.36±0.14	0.51±0.05	0.82±0.06
Kidney	2.52±0.12	0.89±0.06	0.31±0.14	0.65±0.09	0.89±0.02
Heart	0.54±0.01	0.25±0.02	0.12±0.04	0.20±0.01	0.28±0.02
Small intestine	0.84±0.12	0.47±0.10	0.22±0.03	0.39±0.04	0.58±0.13
Striatum/cerebellum	1.65	5.7	12	5.0	1.2
Striatum/cerebral cortex	1.13	3.3	12	3.75	0.86
Brain/blood	1.18	0.57	0.63	0.6	0.29

a) Expressed as %dose/g with the mean ± S.D. of three rats. b) 0.8mmol/kg of haloperidol was injected intravenously 30 min before injection of the radiolabeled ligand.

The inhibition of the striatal uptake of [ $^{18}\text{F}$ ]2 was carried out with the use of haloperidol as a competitive ligand. A saline solution containing 0.8 mmol/kg of haloperidol, which dosage was already shown to be enough to inhibition,<sup>1)</sup> was injected into rat tail veins 30 minutes before the injection of a saline solution of [ $^{18}\text{F}$ ]2. Its tissue distribution at 30 minutes after the injection are listed in Table 2. The uptake of [ $^{18}\text{F}$ ]2 in the striatum was much inhibited to 20% of control, resulting in the smaller striatal/cerebellar ratio of 1.2. Thus, the uptake inhibition by haloperidol clearly demonstrated the specific binding of [ $^{18}\text{F}$ ]2 to CNS dopamine D2 receptors.

In conclusion, [ $^{18}\text{F}$ ]fluorinated benzofuran derivative ([ $^{18}\text{F}$ ]2) exhibited relatively high striatal/cerebellar radioactivity ratio, and may be a suitable ligand for *in vivo* PET radiotracer study of dopamine D2 receptors.

- 1) a) T. Fukumura, H. Dohmoto, M. Maeda, E. Fukuzawa, and M. Kojima, *Chem. Pharm. Bull.*, **38**: 1740 (1990), b) K. Watanabe, T. Fukumura, S. Sasaki, M. Maeda, and S. Takehara, *ibid*, **39**: 3211 (1991), c) M. Maeda, S. Sasaki, T. Fukumura, E. Fukuzawa, K. Watanabe, M. Kojima, T. Tahara, K. Masuda, and Y. Ichiya, *ibid*, **40**: 1793 (1992).
- 2) S. Sasaki, F. Takao, K. Watanabe, N. Obana, M. Maeda, T. Fukumura, S. Takehara, *ibid*, **41**: 296 (1993).



**Preparation and Evaluation of  $^{76}\text{Br}$ -FLB 457,  $^{76}\text{Br}$ -FLB 463 and  $^{76}\text{Br}$ -NCQ 115, Three Selective Benzamides for Mapping Dopamine D2 Receptors with PET.**

LOCH, C.; HALLDIN\*, C.; BOTTLAENDER, M.; SWAHN\*, C.G.; MORESCO, R.M.; MAZIERE, M.; FARDE\*, L.; and MAZIERE, B. Service Hospitalier Frédéric Joliot, CEA, F-91406 Orsay France; \* Department of Psychiatry and Psychology, Karolinska Institute, S-10401 Stockholm, Sweden.

FLB 457 the bromo analogue of epidepride: [(S)-5-bromo-N-((1-ethyl-2-pyrrolinidyl)-methyl)-2,3-dimethoxybenzamide], FLB 463 the bromo analogue of NCQ 298: [(S)-5-bromo-N-((1-ethyl-2-pyrrolinidyl)-methyl)-5,6 dimethoxysalicylamide] and NCQ115 [(+)-(R)-5 bromo-N((1-(4-fluorobenzyl)-2-pyrrolidinyl)-methyl)-2,3-dimethoxybenzamide] are three potent dopamine D2 receptor antagonists that inhibit the  $^3\text{H}$ -spiperone binding in nanomolar concentrations (1,2). FLB 457 and NCQ 115 have been labelled with  $^{11}\text{C}$  and  $^{18}\text{F}$  respectively and used for PET analysis of central D2 receptors (3,4). To investigate the kinetics of FLB 457, FLB 463 and NCQ115 for a long time period, these three bromobenzamides have been labelled with  $^{76}\text{Br}$  ( $T_{1/2} = 16.2\text{h}$ ).

$^{76}\text{Br}$ -FLB 457 and  $^{76}\text{Br}$ -NCQ 115 were prepared by a electrophilic substitution of the tributyl-tin precursor (150 $\mu\text{g}$ ). The exchange between nca  $^{76}\text{Br}$  (200 MBq) and the leaving group occurred in 30 min at room temperature in presence of peracetic acid (100  $\mu\text{L}$  acetic acid, 50  $\mu\text{L}$  hydrogen peroxide) (5).  $^{76}\text{Br}$ -FLB 463 has been prepared by a direct electrophilic substitution enhanced by the hydroxy group of the debromo analogue using the same oxydating conditions. The purification of the  $^{76}\text{Br}$ -FLB 457 was performed by semi-preparative straight phase HPLC using a mixture of chloroform-methanol as eluent with a total radiochemical yield of 80%. The purifications of  $^{76}\text{Br}$ -NCQ 115 and  $^{76}\text{Br}$ -FLB 463 were performed on a semi-preparative reverse phase HPLC using a mixture 0.01M phosphoric acid-acetonitrile as eluent with radiochemical yields of 60 and 50% respectively. Radiochemical and chemical purities of the radioligands assessed by radio-TLC and HPLC were 99% with a specific radioactivity of 40 GBq/ $\mu\text{mol}$ .

In vivo biodistribution studies in rats showed a high uptake of  $^{76}\text{Br}$ -FLB 457 in the striatum (2 % ID/g). The striatum/cerebellum radioactivity concentration ratios were 38, 60 and 120, at 2, 3 and 6 h after injection. Radioactivity in the striatum was almost completely displaced ( $S/C = 6$  at 3 h) after injection of a cold load of 1 mg/kg of raclopride thus demonstrating the specificity and reversibility of  $^{76}\text{Br}$ -FLB 457 binding to dopamine D2 receptors. Radio TLC metabolite analysis indicated that  $^{76}\text{Br}$ -FLB 457 was rapidly metabolised in plasma. In the striatum, 24 h after injection, 95% of the radioactivity still represented unchanged radiotracer. In PET studies in baboons,  $^{76}\text{Br}$ -FLB 457 and  $^{76}\text{Br}$ -FLB 463 showed rapid and high uptakes in the striatum; these radioactivity concentrations reached a plateau 1 h after injection (1.2 and 0.6  $10^{-3}$  ID/g respectively) (fig. 1). Due to the constant wash-out in the cerebellum, the striatum to cerebellum radioactivity concentration ratio values ( $S/C$ ) increased from 12, 1 h p.i., to 28, 4 h p.i. for  $^{76}\text{Br}$ -FLB 457. At the same imaging times, the  $^{76}\text{Br}$ -FLB 463  $S/C$  values were 10 and 21 respectively. Metabolite analysis in plasma samples showed that, 4 h post injection of  $^{76}\text{Br}$ -FLB 457 and  $^{76}\text{Br}$ -FLB 463, 25% and 15% of the radioactivity were related to unchanged compounds. The relative stability of FLB 457 compared to that of FLB 463 could explain the higher striatal uptake observable with FLB 457.

$^{76}\text{Br}$ -FLB 457 which has a very high in vivo uptake, a reversible in vivo binding and a high contrast with extra striatal structures, appears to be a potential ligand for clinical PET studies of brain D-2 receptors in human.

1. Högberg T., de Paulis T., Johansson L. et al, J. Med. Chem. **33**: 2305 (1990)
2. Högberg T, Mohell N. and Ström P. Acta Pharm. Nord. **4**: 297 (1992)
3. Halldin C., Högberg T., Hall H. et al, J. Lab Comp. Radiopharm. **22**: 282 (1993)

4. Halldin C., Högberg T., Bengtsson S. et al, J. Lab Comp. Radiopharm. 30:355 (1991)
5. Mazière B., Loc'h C., Stulzaft O., et al, Eur. J. Pharmacol. 127: 239 (1986)

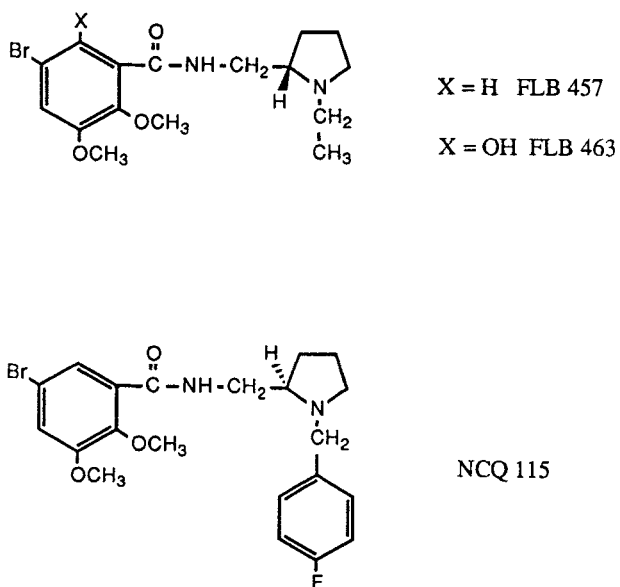
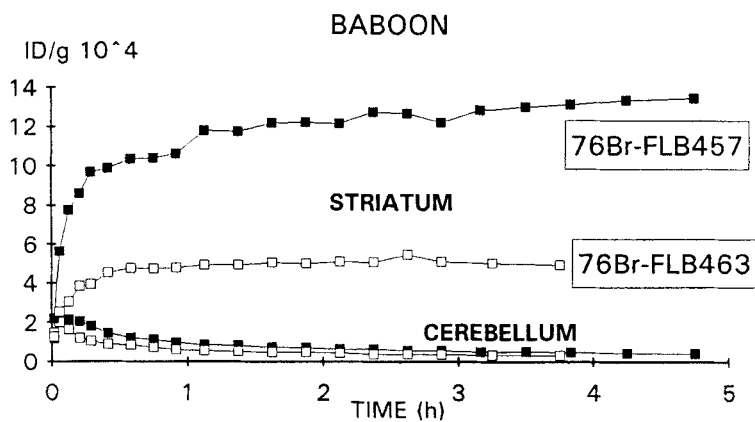


figure 1



**Structure-Activity Relationships of Dopamine Transporter Ligands: Stereospecificity in Binding of 2 $\beta$ -carbomethoxy-3 $\beta$ -Phenyltropane Analogs**

BALDWIN; R.M.; LARUELLE; M.; SCANLEY; B.E.; AL-TIKRITI; M.; ZEA-PONCE, Y., ZOGHBI, S.S., CHARNEY, D.S., HOFFER, P.B., WANG\*, S., GAO\*, Y., NEUMEYER\*, J.L., and INNIS, R.B. Department of Psychiatry and Diagnostic Radiology, Yale University, West Haven, CT 06516, and Research Biochemicals, International, Natick MA 01760, USA.

A key step in neurotransmission is reuptake of dopamine, mediated by the dopamine transporter located on the presynaptic terminal. A radiolabeled probe of the dopamine transporter would be useful in studying the mechanism of cocaine addiction as well as following neurological conditions such as Parkinson's disease. Among the most potent ligands for the dopamine transporter are analogs of 2 $\beta$ -carbomethoxy-3 $\beta$ -phenyltropane (CPT or WIN 35,065-2) (1) and its 4-fluorophenyl analog (CFT or WIN 35,428) (2). In this study we relate the structure of a series of iodinated phenyltropane analogs to their properties with respect to pharmacological specificity for the dopamine transporter *in vitro* and *in vivo* and their pharmacokinetics in primates.

The key intermediate 2 $\beta$ -carbomethoxy-3 $\beta$ -phenyltropane was synthesized from anhydroecgonine methyl ester by Grignard addition to form a mixture of C-2 epimeric phenyltropane carboxylic esters which were separated by column chromatography. The C-2 $\beta$  or (1*R*,2*S*,3*S*) configuration corresponding to (-)-cocaine was elaborated into a) derivatives substituted on the phenyl ring by electrophilic substitution and derivatization; b) *N*-substituted analogs by *N*-demethylation with ACE-Cl followed by alkylation with the appropriate alkyl halide; and c) ester analogs by hydrolysis of the ester and esterification with the appropriate alcohol. The compounds were screened for dopaminergic activity *in vitro* by measuring their ability to displace [<sup>3</sup>H]CFT or [<sup>125</sup>I] $\beta$ -CIT from rat caudate. The most promising candidates were labeled with radioiodine via their 4-trialkylstannylphenyl derivatives, synthesized from the corresponding 4-iodophenyl compound by reaction with the hexaalkyldistannane in the presence of a Pd (0) catalyst. The labeled products were prepared by iododestannylation with peracetic acid for 20-30 min at room temperature and pH 3 and purified by HPLC on C-18 reversed phase with MeOH/H<sub>2</sub>O/Et<sub>3</sub>N (75/25/0.2) at 1.0 mL/min, achieving radiochemical purity > 97% in all cases. *In vivo* binding to the dopamine transporter was assessed in baboons by SPECT imaging. Plasma metabolites were measured by solvent extraction and HPLC.

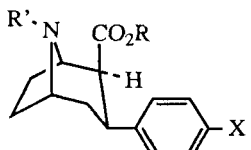
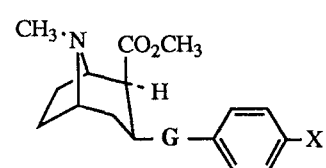
Most of the derivatives tested (Table 1) had less affinity for the dopamine transporter than cocaine (4g). Substitution of the 3 $\beta$ -benzoyl ester moiety by a carbamate ester linkage (4a-e), or benzyloxy (4f) linkage destroyed binding affinity. Modification of the 2 $\beta$ -carboxylate ester and the *N*-alkyl group proved more forgiving, with compounds having IC<sub>50</sub> values in the nanomolar range. As previously reported (3, 4), compound 1b, 2 $\beta$ -carbomethoxy-3 $\beta$ -(4-iodophenyl)tropane ( $\beta$ -CIT) was among the most potent candidates.

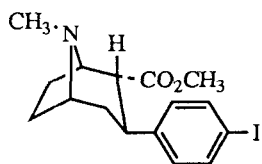
The stereochemical requirements are illustrated by the modifications to the  $\beta$ -CIT structure, which shares the configuration of (-)-cocaine, that is (1*R*,2*S*,3*S*). Inversion of configuration at the 2-position resulted in reduced affinity; the 2 $\alpha$  or (1*R*,2*R*,3*S*) epimer 5 was about 1000 times less potent. The enantiomer (1*S*,2*R*,3*R*) or (1*S*)- $\beta$ -CIT 6 was essentially devoid of activity. In saturation binding experiments with [<sup>125</sup>I] labeled ligands, the total binding of the inactive isomer 6 in the striatum (0.18 pM) was equivalent to the nonspecific binding of the active isomer (0.17 pM). *In vivo* localization determined by SPECT imaging of the I-123 labeled tracers in baboons mirrored the *in vitro* results. In contrast to the high and specific uptake of [<sup>123</sup>I](1*R*)- $\beta$ -CIT, which showed stable striatum:cerebellum ratios of 5-7 over several hours and was > 75 % displaced by 1  $\mu$ mol/kg nonradioactive (1*R*)- $\beta$ -CIT (5), the inactive isomer [<sup>123</sup>I](1*S*)- $\beta$ -CIT brain uptake peaked within 20 min, washed out 10 x faster than the (1*R*) isomer, and was not displaced by carrier (1*R*)- $\beta$ -CIT, even after prolonged infusion of the radiotracer. The peripheral metabolism, however, was unaffected, with similar plasma clearance rates of 145 and 155 L/h, respectively (6). On the other hand, the isopropyl ester analog of (1*R*)- $\beta$ -CIT 3b, which had similar *in vitro* binding and *in vivo* uptake, had a reduced rate of peripheral metabolism, with plasma clearance of 99 L/h.

## References

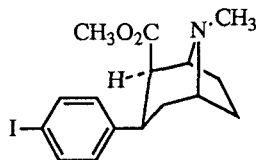
1. Clarke R.L., Daum S.J., Gambino A.J., *et al.* - *J. Med. Chem.* **16**: 1260 (1973).
2. Madras B.K., Spealman R.D., Fahey M.A., *et al.* - *Mol. Pharmacol.* **36**: 518 (1989).
3. Neumeyer J.L., Wang S., Milius R.A., *et al.* - *J. Med. Chem.* **34**: 3144 (1991).
4. Innis R., Baldwin R., Sybiraska E., *et al.* - *Eur. J. Pharmacol.* **200**: 369 (1991).
5. Laruelle M., Baldwin R.M., Malison R.T., *et al.* - *Synapse* **13**: 295 (1993).
6. Baldwin R.M., Zea-Ponce Y., Zoghbi S.S., *et al.* - *Nucl. Med. Biol. - Int. J. Rad. App. B* **20**: 597 (1993).

**Table 1.** Binding affinity of derivatives of 2 $\beta$ -carbomethoxy-3 $\beta$ -phenyltropane to rat caudate tissue (inhibition of [<sup>3</sup>H]CFT or [<sup>125</sup>I] $\beta$ -CIT)

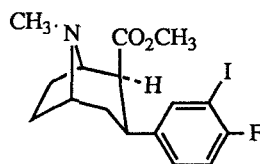
				IC <sub>50</sub> (nM)			
R	R'	X		G	X	IC <sub>50</sub> (nM)	
<b>1a</b>	CH <sub>3</sub>	CH <sub>3</sub>	F		H	>1000	
<b>b</b>			I		F	>1000	
<b>c</b>			CF <sub>3</sub>		Cl	>1000	
<b>2a</b>	CH <sub>3</sub>	H	F		OCH <sub>3</sub>	>1000	
<b>b</b>		CH <sub>3</sub>	F		N <sub>3</sub>	>1000	
<b>c</b>		CH <sub>3</sub> CH <sub>2</sub> CH <sub>2</sub>	F				
<b>d</b>		CH <sub>2</sub> =CHCH <sub>2</sub>	F				
<b>e</b>		<i>p</i> -IC <sub>6</sub> H <sub>4</sub> CH <sub>2</sub>	I				
<b>3a</b>	CH <sub>2</sub> CH <sub>3</sub>	CH <sub>3</sub>	I	<b>4f</b>	OCH <sub>2</sub>	H	>1000
<b>b</b>	CH(CH <sub>3</sub> ) <sub>2</sub>	CH <sub>3</sub>	I	<b>g</b>	OCO	H	221 ± 14



**5**  
IC<sub>50</sub> 340 ± 120 nM



**6**  
IC<sub>50</sub> >1000 nM



**7**  
IC<sub>50</sub> 86 ± 5 nM

**SYNTHESIS OF [<sup>18</sup>F] RP 62203, A SELECTIVE ANTAGONIST OF 5HT<sub>2</sub> RECEPTORS FOR POSITRON EMISSION TOMOGRAPHY STUDIES.**

LASNE M.C.; LE SECQ B.; BARRE L.+; COLLINS M; HUARD C ; and BARON J. C.++

Unité de Recherche Associée au CNRS , Institut des Sciences de la Matière et du Rayonnement, 6 Bd du Maréchal Juin, 14050 Caen - Université de Caen-Basse Normandie ; +CEA, DSV/DPTE, ++ U INSERM 320 Centre Cyceron, Bd Henri Becquerel, 14021 Caen, FRANCE

The neurotransmitter, 5-hydroxytryptamine (serotonin, 5HT) is thought to play a role in a wide variety of central nervous system functions, including sleep, appetite, mood and pain perception. Understanding this role has led to the search of selective ligands for the different 5-HT receptor subtypes. Several of them have been labelled for PET studies<sup>1</sup>. [<sup>18</sup>F] Setoperone<sup>2</sup> and [<sup>18</sup>F]altanserine<sup>3</sup> with K<sub>i</sub> values of 0.37 and 0.16 nM are presently the only two radioligands that are used in PET to study the 5-HT<sub>2</sub> receptors.

Recently, RP 62203 (2-[3-(4-(4-fluorophenyl)-piperazinyl)propyl]-naphto[1,8-cd]isothiazole -1,1- dioxide), was described<sup>4</sup> and found to be one of the most potent and highly selective serotoninergic 5-HT<sub>2</sub> receptor antagonist described to date<sup>5, 6</sup>. It binds potently to the 5-HT<sub>2</sub> receptor with a K<sub>i</sub> value of 0.26 nM which is about 100 and 300 lower than that for the 5-HT<sub>1A</sub> and 5-HT<sub>1C</sub> sites respectively. Its labelling with a positron emitter should be useful in evaluating *in vivo* the role of these receptors in serotonin-mediated neurotransmission in the central nervous system.

A rapid synthesis of N,N'-disubstituted piperazines was described<sup>7</sup> and successfully applied to the preparation of N -1-(4-[<sup>18</sup>F]-fluorophenyl)piperazine. The alkylation of this latter with the appropriate chloride in DMF gave [<sup>18</sup>F] RP 62203 in 7-15 % radiochemical yield (decay corrected). Due to a long reaction time (overall synthesis time : 145 - 165 min), the routine preparation of [<sup>18</sup>F] RP 62203 could not be envisaged. We report here an improvement of the synthesis of [<sup>18</sup>F] RP 62203 based on the rapid condensation of the bis(bromoethylamine)derivative 3 with fluoroaniline 2.

The N-(3-chloropropyl)-naphtosultam 4 was prepared<sup>4</sup> from the commercially available naphtosultam. Its alkylation with bis(2-hydroxyethyl)amine in DMF in the presence of triethylamine yielded the diol 5 in 55 % yield. Reaction of this latter with carbontetrabromide and triphenylphosphine<sup>8</sup> in dichloromethane at 0°C for 30 min gave the dibromide 3 after work up and purification by a rapid chromatography on silica gel.

Optimization of a previously described method<sup>9</sup> allowed us to prepare [<sup>18</sup>F] fluoroaniline 2 (as free base) in 35 - 60 % yield and in less than 30 min from [<sup>18</sup>F] fluoride. The reaction of 2 with the dibromide 3 was studied under different conditions (time, temperature, microwave activation, solvent, base, amount of reagents, dilution). Analysis of the crude reaction mixture by radio-TLC showed that the expected compound 1 was the main product of the reaction (50-60% of the total radioactivity) when the reaction was carried out for 4 min in butanol at 150°C (or for 6 min in octanol at 150°C) in the presence of sodiumhydrogenocarbonate. It was contaminated by an unidentified polar side-product (R<sub>f</sub> : 0 under the TLC conditions shown in Table 1). The ratio of this compound was strongly dependent on the reaction time and on the purity of the starting bis(bromoethyl)amine. No improvement in the yield of 1 was observed when using either the bismesylate of the diol 5 instead of the dibromide 3 or microwave activation. No reaction was observed in dipolar aprotic solvents (DMSO, DMF).

After reaction, the crude reaction mixture was passed through a sep-pak (silica) and the compound **1** eluted with dichloromethane. The residue obtained after evaporation of the solvents, was injected onto a reverse phase HPLC column (table 1). [ $^{18}\text{F}$ ]RP was isolated in 30-40 % yield (decay corrected) from [ $^{18}\text{F}$ ] fluoroaniline and in 10 - 21 % overall yield from [ $^{18}\text{F}$ ] fluoride with a total synthesis time of 65 min.

The synthesis is now being automated for the preparation of injectable amounts of [ $^{18}\text{F}$ ] RP 62203 and for the *in vivo* studies of its biodistribution and pharmacokinetics.

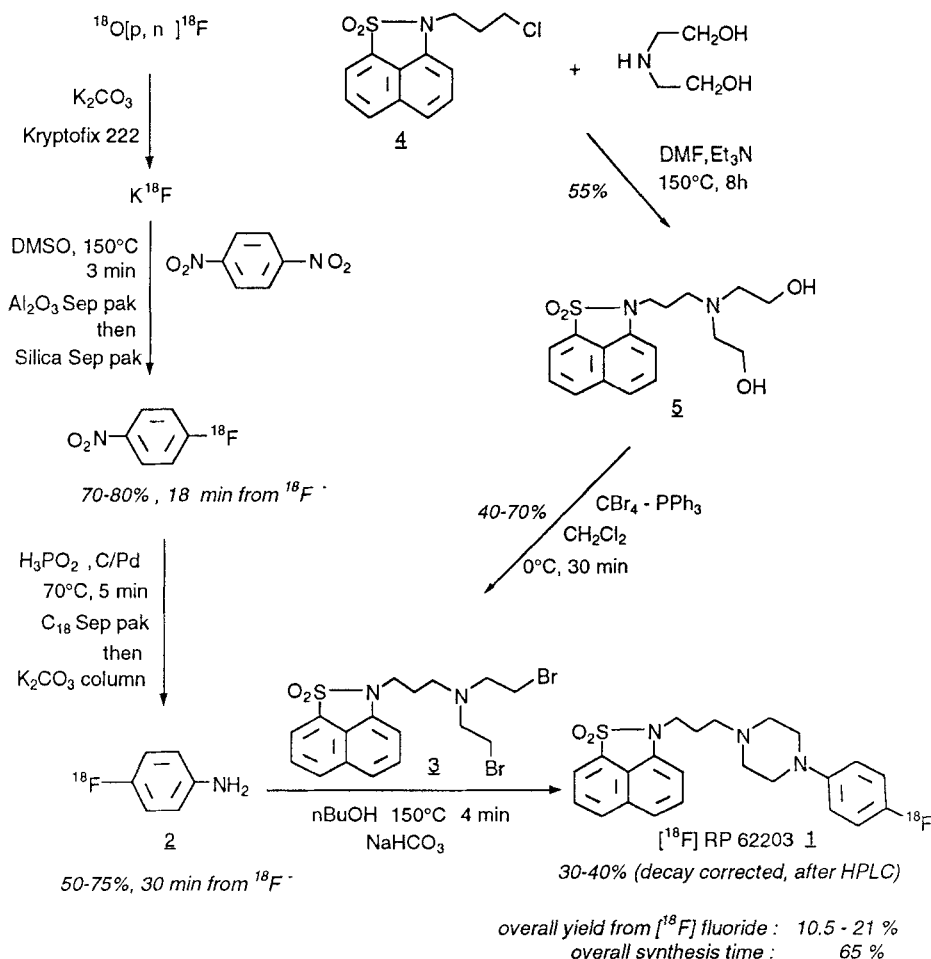
Scheme 1 : radiosynthesis of [ $^{18}\text{F}$ ] RP 62203

Table 1 : characterization of [<sup>18</sup>F] RP 62203 1 by HPLC or TLC

HPLC <sup>(a)</sup> eluent	retention time (min)		TLC <sup>(d)</sup> eluent	Rf	
	<u>1</u>	<u>2</u>		<u>1</u>	<u>2</u>
AcOEt: heptane (60: 40, v/v) <sup>(b)</sup>	14	7	AcOEt: heptane (60: 40, v/v)	0.30	0.56
H <sub>2</sub> O: MeCN : NEt <sub>3</sub> (50: 40: 0.05, v/v/v) <sup>(c)</sup>	15	6.5	CH <sub>2</sub> Cl <sub>2</sub> : MeOH (98: 2, v/v)	0.44	0.70
MeOH: H <sub>2</sub> O: AcONH <sub>4</sub> (5 mmol.l <sup>-1</sup> ; 70: 30, v/v) <sup>(c)</sup>	9.5	5.5	CH <sub>2</sub> Cl <sub>2</sub> : AcOEt (94: 6, v/v)	0.20	0.46

(a)  $\lambda$  : 254 nm; flow rate : 2 ml.min<sup>-1</sup> ; (b)  $\mu$  Porasil (i.d x l : 8 x30 mm) ; (c) C<sub>18</sub> - $\mu$  Bondapack (i.d x l : 8 x 30 mm) ; (d) silica gel plate

## References

1. Crouzel C., Guillaume M., Barré L., Lemaire C. and Pike V; W. - Nucl. Med. Biol. 19: 857 (1992) and ref. therein
2. Mazière B., Crouzel C., Venet M., Stulzaft O., Sanz G., Ottaviani M., Sejourne C., Pascal O., and Bisserbe J. C. - Nucl. Med. Biol. 15: 463 (1988)
3. Sadzot B., Lemaire C., Cantineau R., Salmon E., Plevenaux A., Maquet P., Hermanne J. P., Franck G., and Guillaume M. - J. Nucl. Med. 31: 1584 (1990)
4. Malleron J. L., Comte M. T., Gueremy C., Peyronel J. F., Truchon A., Blanchard J. C., Doble A., Piot O., Zundel J. L., Huon C., Martin B., Moutton P., Viroulaud A., Allam D., and Betschart J. - J. Med. Chem. 34: 2477 (1991)
5. Doble A., Girdlestone O., Piot D., Allam J., Betschart J., Boireau A., Dupuy C., Guérémy C., Ménager J., Zundel J. L., and Blanchard J. C. - Br. Pharmacol. 105: 27 (1992)
6. Fajolles C., Boireau A., Ponchant M., and Laduron P. - Eur. J. Pharmacol. 216: 53 (1992)
7. Collins M., Lasne M.C., and Barré L. - J. Chem. Soc. Perkin I 3185 (1992)
8. Kocienski P. J., Cernigliaro G., and Feldstein G. - J. Org. Chem. 42: 353 (1977)
9. Shiue C. Y., Watanabe M., Wolf A. P., Fowler J. S., and Salvadori P. - J. Labelled Compd. Radiopharm. 21: 533, 1984